Chromatographic Purification and Labeling of Canine Parvovirus

Pro gradu-tutkielma

Jyväskylän yliopisto

Bio- ja ympäristötieteiden laitos

Molekyylibiologian osasto

Kesäkuu 2008

Anne Vaarala

Preface

Tämä pro gradu -tutkielma tehtiin Jyväskylän yliopiston bio- ja ympäristötieteiden laitoksella molekyylibiologian osastolla vuosien 2007 - 2008 aikana. Haluan kiittää Maija Vihinen-Rantaa mahdollisuudesta osallistua tähän tutkimukseen.

Erityiset kiitokset haluan osoittaa ohjaajalleni Teemu Ihalaiselle, jota ilman en koskaan olisi saanut tutkimustani valmiiksi. Haluan myös kiittää Einari Niskasta hyvistä neuvoista matkani varrella.

Lisäksi minun on osoitettava kiitokseni Outi Paloheimolle, jonka kanssa olen viettänyt monet rattoisat hetket niin laboratorion sisä- kuin ulkopuolellakin. Haluan kiittää myös muita molekyylibiologian osaston ihmisiä kannustavasta ilmapiiristä. Suuret kiitokset myös ystävilleni, jotka ovat jaksaneet kuunnella minua ahdistuksen hetkinä.

Lopuksi haluan osoittaa kiitokseni äidilleni ja siskolleni, jotka ovat jaksaneet uskoa minuun koko opiskeluaikani.

Jyväskylän yliopisto
Matemaattis-luonnontieteellinen tiedekunta

Pro gradu – tutkielman tiivistelmä

Tekijä: Anne Vaarala
Tutkielman nimi: Koiran parvoviruksen kromatografinen puhdistus ja leimaaminen
English title: Chromatographic Purification and Labeling of Canine Parvovirus
Päivämäärä: 6.6.2008 **Sivumäärä:** 51

Laitos: Bio- ja ympäristötieteiden laitos
Oppiaine: Molekyylibiologia
Tutkielman ohjaajat: FM Teemu Ihalainen, dosentti Maija Vihinen-Ranta

---

Tiivistelmä:

Koiran parvoviruksen (CPV) kapsidi on läpimitaltaan 26 nm ja sen isoelektrinen piste on 5.3 pH, jolloin sillä on negatiivinen varaus neutraalissa ympäristössä.

CPV:n puhdistuksessa on yleisesti käytetty cesiumkloridi (CsCl)-gradienttiin perustuvaa sentrifugaatiota, jonka on todettu vähentävän viruksen infektiivisyyttä. Tämän vuoksi on ollut tarpeen kehittää uusia puhdistusmentelmiä, joilla ei olisi haitallisia vaikutuksia CPV:n kykyyn infektoida soluja.

Tämän tutkimuksen tarkoituksena oli luoda sopiva puhdistusprotokolla koiran parvovirukselle käyttäen kokoon perustuvaa kromatografaa ja anionin- ja kationinvaihtovaihtokromatografiaa. Lisäksi puhdistettuja CPV kapsideja oli tarkoitus leimata fluoresoivaksi, jotta niiden kulkua solussa voitaisiin seurata. Tällä tavoin voitaisiin havainnoida puhdistuksen vaikutusta viruksen infektiivisyyteen. Puhdistusmenetelmän vaikutusta viruksen infektiivisyyteen oli myös tarkoitus tutkia infektiokokeiden avulla. Tarkoituksena oli lisäksi konjugoida puhdistettuihin CPV-kapsideihin fluoresoiva leima, jolloin viruksen kulkua solussa voitaisiin havainnoida konfokaalimikroskoopin avulla. Lopuksi puhdistettua virusta oli tarkoitus tutkia atomivoimamikroskoopin (AFM) avulla.

Tutkimuksessa selvisi, että anioninvaihtokromatografia on yksinään riittävä menetelmä erottelemaan CPV-kapsidit muista mediumin proteiineista. Kationinvaihtokromatografia sen sijaan ei ole sopiva menetelmä CPV:n puhdistamiseksi. Lisäksi saimme selville, ettei kromatografinen puhdistus heikennä CPV:n kykyä infektoida NLFK-soluja. Yrityksemme konjugoida Alexa tai Atto-värejä puhdistettuihin CPV kapsideihin valitettavasti epäonnistui.

Avainsanat: koiran parvovirus, kromatografia, puhdistus

University of Jyväskylä
Faculty of Mathematics and Science

Abstract of Master´s Thesis

Author: Anne Vaarala
Title of thesis: Chromatographic Purification and Labeling of Canine Parvovirus
Finnish title: Koiran parvoviruksen kromatografinen puhdistus ja leimaaminen
Date: 6.6.2008 **Pages:** 51

Department: Department of Biological and Environmental Science
Chair: Molecular Biology
Supervisors: M.Sc. Teemu Ihalainen, Docent Maija Vihinen-Ranta

---

Abstract:

Canine parvovirus (CPV) nonenveloped capsid is roughly 26 nm in diameter and has an isoelectric point of 5.3 pH which makes the capsid negatively charged at neutral pH.

Currently the purification process of CPV involves cesium chloride gradient centrifugation which is known to reduce the infectivity of the capsids. Consequently there has been an increasing interest in developing novel methods for the purification of CPV capsids with higher quality.

The aim of this study was to develop a purification protocol for canine parvovirus using chromatographic methods. Additionally, the purified capsids would be labeled with fluorescent dyes in order to detect the infection process inside the cells using confocal microscopy. Infection studies would be carried out to find out whether the purification protocol has unfavorable effects on the infectivity of the virus. Finally, the purified capsids would be detected using atomic force microscopy (AFM) to examine the effectiveness of the purification protocol.

It was discovered that anion exchange chromatography alone is adequate to separate CPV capsids from other proteins present in the medium. Cation exchange chromatography instead is not suitable for CPV purification. We also found out that chromatographic purification does not prevent CPV capsids from infecting NLFK cells. Our effort of conjugating fluorescent Alexa or Atto dyes to CPV capsids did unfortunately not succeed.

Keywords: canine parvovirus, chromatography, purification

Table of Contents

ABBREVIATIONS

AFM	atomic force microscope
CPV	canine parvovirus
CsCl	cesium chloride
DMEM	Dulbecco's modified Eagle's medium
FPV	feline panleukopenia virus
NLFK	Nordon laboratory feline kidney
NS	non-structural viral protein
ORF	open reading frame
PBS	phosphate-buffered saline
PFA	paraformaldehyde
p.i.	post infection
SDS-PAGE	sodium dodecyl sulfate polyacrylamide gel electroforesis
TBS	Tris-buffered saline
VP	(structural) viral protein

1 INTRODUCTION

1.1 Canine Parvovirus

1.1.1 Background

Canine parvovirus (CPV) suddenly emerged in the mid-1970s and during 1978 it was recognized as the cause of a new disease in dogs throughout the world (reviewed by Parrish, 1990). The original virus strain was called CPV type 2, but between 1979 and 1982 it was replaced by a new antigenic type called CPV type 2a (Parrish *et al*., 1988). Around 1984 another CPV strain called CPV type 2b emerged and by 1988 it was the predominant type (Parrish *et al*., 1991). There is evidence of a novel CPV strain, referred to as CPV type 2c, which has become widely distributed since its discovery in 2000 (Buonavoglia *et al*., 2001; Decaro *et al*., 2005; Pérez *et al*., 2007).

CPV belongs to the feline subgroup of the genus *Parvovirus* within the family *Parvoviridae* (reviewed by Parrish, 1990). CPV is closely related to feline panleukopenia virus (FPV) and to the other autonomous parvoviruses that infect carnivores (Reed *et al.*, 1988; Martyn *et al.*, 1990; Truyen *et al.*, 1995). Phylogenetic studies of CPV proteins show that CPV strains evolved from a common ancestor which could have been FPV or some other closely related virus (Truyen *et al*., 1995; Horiuchi *et al.*, 1998). CPV and FPV differ in their antigenic and hemagglutination properties (reviewed by Parrish, 1990; Chang *et al*., 1992; Llamas-Saiz *et al.*, 1996) as well as in their host range (reviewed by Parrish, 1990; Steinel *et al*., 2001).

1.1.2 Host Range

CPV and FPV have distinct host ranges both *in vitro* and *in vivo*. CPV can replicate efficiently in canine and feline cell cultures, while FPV replication is restricted to cultured feline cells (Tratschin *et al.*, 1982; Truyen and Parrish, 1992; Hueffer *et al.*, 2003a, b). However, FPV can replicate quite efficiently in the thymus of dogs inoculated with the virus (Truyen and Parrish, 1992). *In vivo*, CPV infects several members of the family Canidae, while FPV infects members of the family Felidae (Parrish *et al.*, 1988; reviewed by Parrish, 1990; Steinel *et al*., 2001). The differences in CPV and FPV host ranges are due to their distinct abilities to bind the canine transferrin receptor (Hueffer *et al.*, 2003a, b). These distinctions are determined by specific amino acids in the capsid protein VP2, on the threefold spike region (Chang *et al*., 1992; Llamas-Saiz *et al*., 1996; Parker and Parrish, 1997; Hueffer *et al.*, 2003a, b; Govindasamy *et al.*, 2003). On the other hand, certain amino acids in the apical domain of the canine transferrin receptor control the binding of CPV and FPV to the cell surface, thus affecting their abilities to infect canine cells (Palermo *et al*, 2003; Palermo *et al.*, 2006).

1.1.3 Genome

CPV has a linear, negative sense single-stranded DNA genome of approximately 5300 nucleotides in length with hairpin-shaped palindromic nucleotide sequences at both termini (Paradiso *et al*., 1982; Reed *et al.*, 1988; reviewed by Cotmore and Tattersall, 2007). A portion (13%) of the genome is displaying icosahedral symmetry and has an unusual conformation with the bases pointing outwards forming several hydrogen bonds with the amino acids of the capsid, while the phosphoribose backbone is pointing inwards, interacting with metal ions (Tsao *et al.*, 1991; Chapman and Rossmann, 1995).

The genome contains two major open reading frames (ORFs) which encode four proteins by alternative mRNA splicing (**Fig. 1**). Nonstructural proteins NS1 and NS2 are made from the first (left hand, 3') and structural proteins VP1 and VP2 from the second (right hand, 5') ORF (Reed *et al*., 1988). VP1 contains the entire amino acid sequence of VP2 as well as additional residues in the amino terminus (Rhode III, 1985; Reed *et al.*, 1988). The VP1 unique region contains several basic amino acids at the amino terminus which have been identified as a nuclear localization signal (Vihinen-Ranta *et al.*, 1997; Vihinen-Ranta *et al.*, 2002). Within the amino terminus of VP1 there is also a phospholipase A2-like domain (Suikkanen *et al.*, 2003b). Both of these VP1 regions are essential for successful CPV infection (Vihinen-Ranta *et al.*, 2002; Suikkanen *et al.*, 2003b). NS1 functions as a replication initiator protein and is needed for viral infection (reviewed by Cotmore and Tattersall, 2007). NS2 does not seem to have an important role in CPV infection nor capsid assembly (Wang *et al.*, 1998).

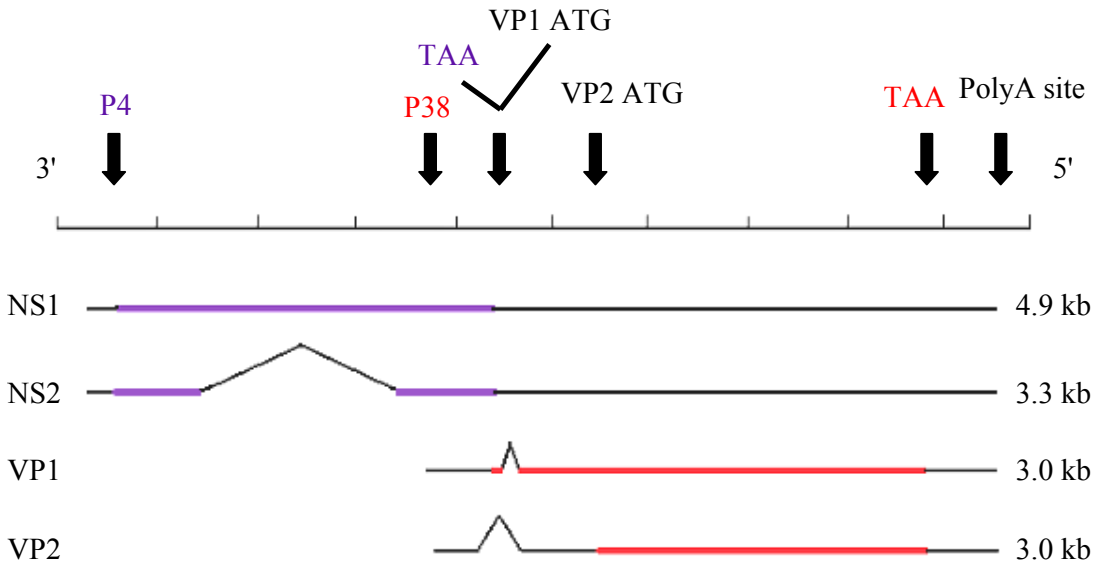

Fig. 1. Transcriptional map of CPV genome. CPV genome is single-stranded, approximately 5300 nucleotides in length and contains two ORFs. Both ORFs encode two mRNAs by alternative splicing. The ORFs have the same polyadenylation site, but they are controlled by different promoters, P4 and P38. The sizes of the major virion mRNAs are indicated on the right, while the encoded proteins are on the left. The genome is represented in 3' → 5' direction. Colored lines represent regions in mRNA that are translated into proteins. (Adapted from the figure by Reed *et al.*, 1988.)

1.1.4 Capsid Structure

CPV nonenveloped capsid is about 26 nm in diameter. It is composed of 60 copies of protein subunits and has T=1 icosahedral symmetry. In DNA-containing (full) virus particles 90 % of the proteins is VP2 and the remaining 10 % is VP1 and VP3 (Tsao *et al.*, 1991). Some of the VP2 have their amino termini on the outside of the DNA-containing capsid, passing through a pore at the fivefold axis of symmetry (Tsao *et al.*, 1991; Langeveld *et al.*, 1993; Xie and Chapman, 1996; Agbandje-McKenna *et al.*, 1998; Weichert *et al.*, 1998), while the VP1 unique region is inside the capsid until it becomes exposed later in the infection process (Weichert *et al.*, 1998; Vihinen-Ranta *et al.*, 2002; Suikkanen *et al.*, 2002; Suikkanen *et al.*, 2003b). VP3 is formed by a proteolytic cleavage reaction of 19 amino acids from the amino terminus of VP2 only in full virions (Paradiso *et al.*, 1982; López de Turiso *et al.*, 1991; Weichert *et al.*, 1998). When expressed alone, VP2

can assemble into empty capsids which are antigenically and structurally very similar to the native CPV capsids (López de Turiso *et al.*, 1992; Saliki *et al.*, 1992; Cortes *et al.*, 1993; Hurtado *et al.*, 1996; Yuan and Parrish, 2001). CPV capsid assembly is thought to occur through trimer intermediates which are transported to the nucleus after their synthesis in the cytoplasm (Xie and Chapman, 1996; Riolobos *et al.*, 2006; reviewed by Cotmore and Tattersall, 2007). CPV particles have an isoelectric point of 5.3 pH indicating that the capsids have a negative charge at neutral pH (Weichert *et al.*, 1998).

CPV capsid surface has several structural features. Five eight-stranded antiparallel β-barrels form a cylindrical structure around the fivefold axes. A small channel spans from the outer shell to the inner core of the capsid in the center of each cylinder. The β-strands forming the barrel are joined by large loops which create the majority of the capsid surface. These loops are responsible for constructing the large protrusions on the threefold axes of symmetry, the threefold spikes. Fivefold axes of symmetry are circulated by a canyon-like depression, and another depression, termed the dimple, can be found at the twofold axes (Tsao *et al.*, 1991; Agbandje *et al.*, 1995; Xie and Chapman, 1996; Agbandje-McKenna *et al.*, 1998). The dimple has the binding site for sialic acid, but it does not seem to be important in the infection process of CPV (Tresnan *et al.*, 1995).

1.1.5 Cell Entry and Transportation to Nucleus

CPV infection begins when the virus binds to transferrin receptor on the cell surface (Parker *et al.*, 2001; Hueffer *et al.*, 2003a; Palermo *et al.*, 2003; Hueffer *et al.*, 2004). Virus particles as well as their bound receptors are then rapidly internalized by dynamin-dependent, clathrin-mediated endocytosis in coated vesicles (Parker and Parrish, 2000; Suikkanen *et al.*, 2003b). Inside the cell CPV capsids enter early endosomes and are soon transported to recycling endosomes and on to late endosomes (Vihinen-Ranta *et al.*, 1998; Suikkanen *et al.*, 2002). Before entering the cytoplasm, CPV capsids can be found in lysosomes where the amino terminal of VP1 is exposed (Weichert *et al.*, 1998; Suikkanen *et al.*, 2002;).

The capsids stay within endosomal vesicles for several hours before they are released into the cytosol (Parker and Parrish, 2000; Vihinen-Ranta *et al.*, 2000; Suikkanen *et al.*, 2002), and the transferrin receptors remain associated with the capsids during this time (Parker *et al.*, 2001; Suikkanen *et al.*, 2003b). The release of CPV capsids from lysosomes is thought to occur through the phospholipase A2-activity of VP1, but this alone does not seem to be sufficient for viral escape into the cytosol (Suikkanen *et al.*, 2003b). CPV capsids are transported to the nucleus through nuclear pore complex. Viral DNA is released in the nucleus without capsid disassembly, but the process is still not fully understood. DNA replication is dependent on cellular S-phase and is carried out using rolling hairpin replication-strategy (reviewed by Vihinen-Ranta *et al.*, 2004; Cotmore and Tattersall, 2007).

CPV-containing endosomal vesicles are trafficked through the cytoplasm along microtubules in a dynein-dependent way (Vihinen-Ranta *et al.*, 1998; Vihinen-Ranta *et al.*, 2000; Suikkanen *et al.*, 2002; Suikkanen *et al.*, 2003a). Intact microtubule network is also required for nuclear transport of the capsids (Vihinen-Ranta *et al.*, 2000; Suikkanen *et al.*, 2003a).

1.2 Chromatography

1.2.1 Chromatography in General

The basis of chromatography is the distribution coefficient (K_d), which defines how a compound distributes itself between two immiscible phases. For two such phases A and B, the value for the coefficient is a constant at a given temperature and it can be calculated by the equation:

$$\frac{\text{concentration in phase A}}{\text{concentration in phase B}} = K_d$$

Effective distribution coefficient is defined as the total amount of a compound present in one phase divided by the total amount present in the other phase. For example, if the distribution coefficient of a substance between phases A and B is 1, and if this substance is distributed between 10 cm^3 of phase A and 1 cm^3 of phase B, the concentration in the two phases will be equal, but the total amount of the substance in phase A will be 10 times the amount in phase B (reviewed by Wilson and Walker, 2000).

Chromatographic systems consist of a stationary phase, which is immobilized, and a mobile phase, which flows over or through the stationary phase. The mobile phase (often called as the eluent) can be liquid or gas, while the stationary phase can be solid, gel, liquid or a mixture of solid and liquid. These phases are chosen so that the compounds to be separated have different distribution coefficients. For example, in ion exchange chromatography, there is ion exchange equilibrium between a stationary ion exchanger and a mobile electrolyte phase. Sample components with the highest solubility in the mobile phase will migrate fastest through the stationary phase. Usually, the stationary phase is attached to a matrix support that is packed into a column and the mobile phase is allowed to flow through the column (column chromatography). There are several different matrix

materials available, the most common ones being agarose, cellulose, dextran, polyacrylamide, polystyrene and silica (reviewed by Wilson and Walker, 2000).

There are several chromatographic techniques that can be used in the purification process of viruses. Separation can be based on the size of the virus particle (size-exclusion chromatography), net charge of proteins on the capsid surface (ion exchange chromatography) or a specific feature on the capsid surface (affinity chromatography) (**Fig. 2**).

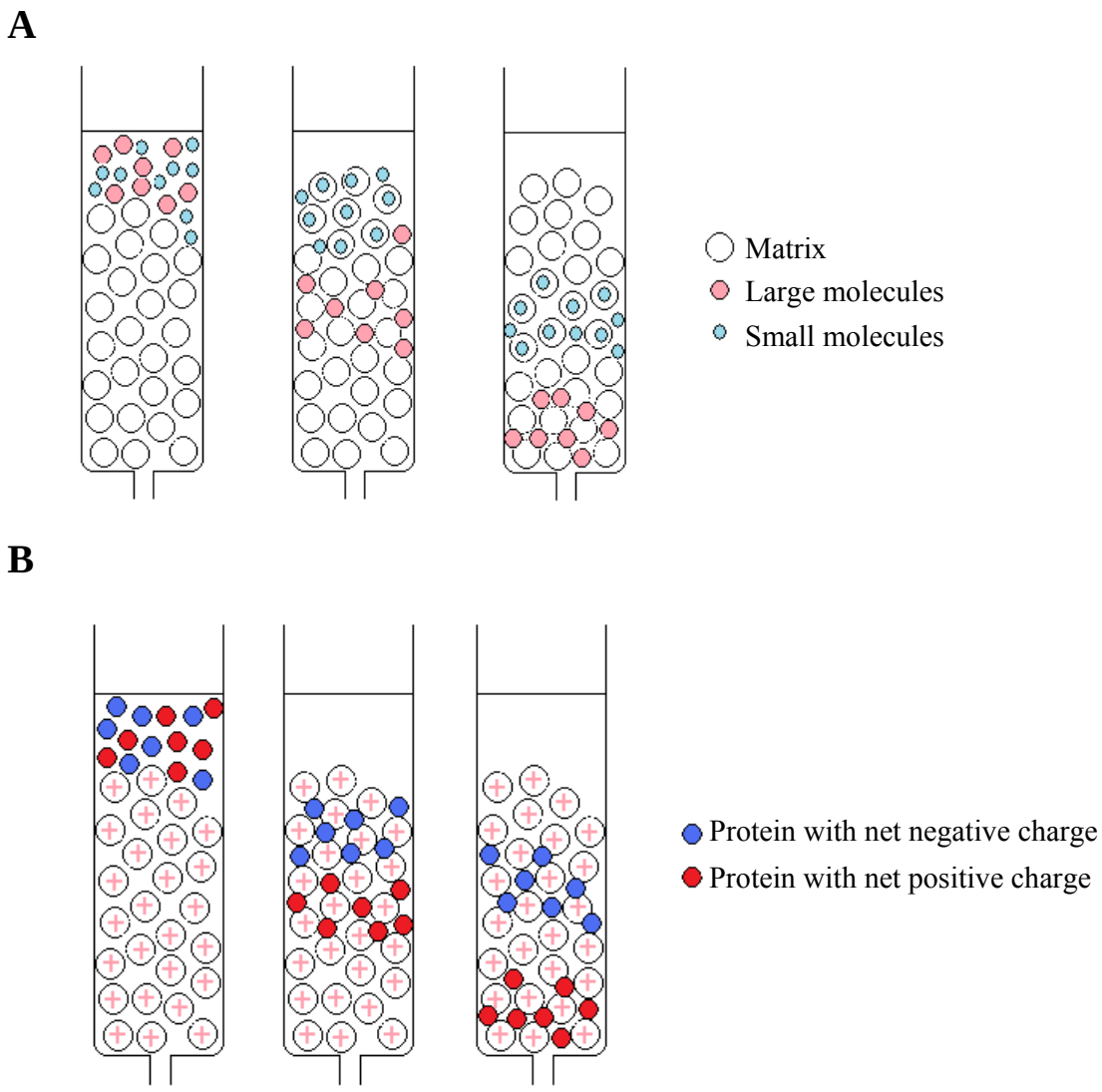

C

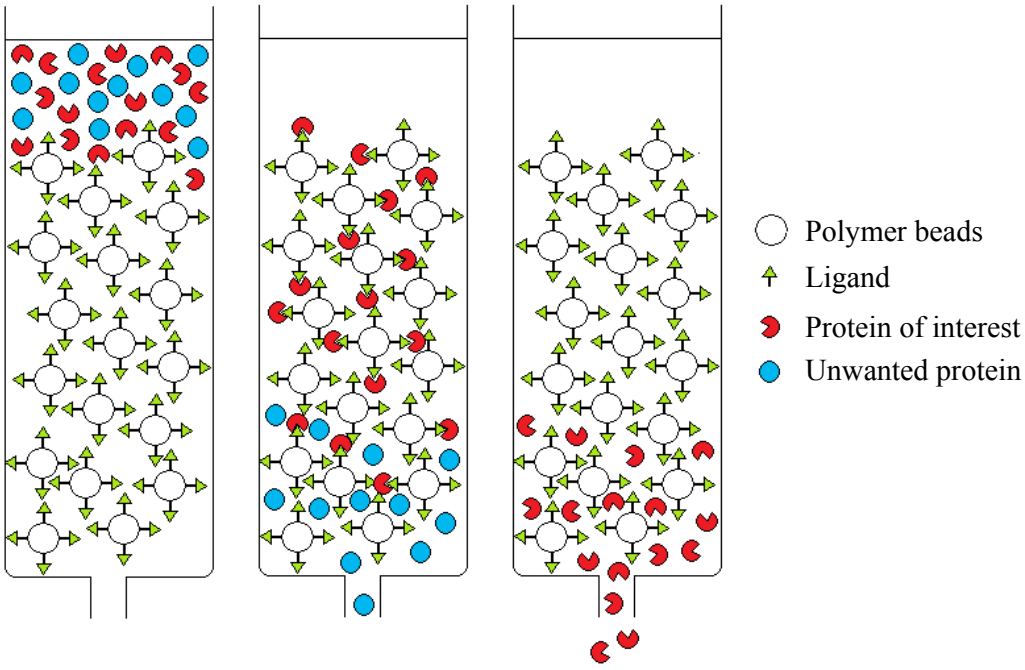

Fig. 2. Different chromatographic techniques. **(A)** Size-exclusion chromatography. The matrix consists of small beads with pores of certain size. Small proteins enter the pores and are slowed down, while large proteins take a more direct route through the column and are eluted first. **(B)** Anion exchange chromatography. The matrix is composed of an organic polymer with positively charged groups attached to it. Negatively charged proteins are attracted to the matrix and migrate much slower through the column than positively charged proteins. **(C)** Affinity chromatography. A ligand specific for the protein of interest is covalently attached to the matrix and is used to bind the target protein. After unwanted proteins are washed away, the protein of interest can be eluted from the column.

Size-exclusion chromatography (also called as gel filtration) separates particles according to their size. The matrix is composed of a cross-linked polymer beads with pores of certain size. Small particles enter the pores and are slowed down, while large particles are unable to enter the pores and migrate rapidly through the column (**Fig. 2A**). Ion exchange matrix usually consists of an organic polymer with charged groups attached to it. These groups can be either positively (anion exchange chromatography) or negatively (cation exchange chromatography) charged and are used to attract molecules of opposite charge (**Fig 2B**). Affinity chromatography is based on a reversible interaction between the target molecule and a specific ligand covalently bound to a chromatography matrix (**Fig. 2C**). This

interaction can be electrostatic or hydrophobic, but it can also result from van der Waals' forces or hydrogen bonding.

1.2.2 Chromatography in Virus Purification

Traditionally CPV purification is performed using cesium chloride (CsCl) gradients which can severely decrease the infectivity of virus particles and are often contaminated with cellular proteins (reviewed by Burova and Ioffe, 2005). Therefore, there has been an increasing interest in developing new methods for purification of virus particles with higher quality and yield. For example, various chromatographic strategies have recently been used in the purification process of recombinant adeno-associated virus which have substantially increased the yield and quality of the purified virus compared to the conventional CsCl gradient-based methods (O'Riordan *et al.*, 2000; Smith *et al.*, 2003; Davidoff *et al.*, 2004; Kamen and Henry, 2004; Duffy *et al.*, 2005; Koerber *et al.*, 2007). Additional improvements of these novel methods compared to the purification processes involving CsCl gradients are their rapidity, simplicity and scalability for commercial purposes (Zolotukhin *et al.*, 1999; O'Riordan *et al.*, 2000; Davidoff *et al.*, 2004; Duffy *et al.*, 2005). Unfortunately, as good as these new methods are, empty virus capsids are difficult, if not impossible, to separate from full virus particles (reviewed by Burova and Ioffe, 2005). These new purification techniques include anion exchange chromatography combined with size-exclusion chromatography (Smith *et al.*, 2003; Kamen and Henry, 2004) and cation exchange chromatography combined with anion exchange chromatography (Davidoff *et al.*, 2004). Chromatographic techniques have also been used recently in the purification processes of other viruses, such as human influenza A virus (Kalbfuss *et al.*, 2007) and retroviruses (Segura *et al.*, 2005; Rodrigues *et al.*, 2007).

In addition to methods utilizing only chromatography, iodixanol gradient combined with heparin affinity chromatography or cation exchange chromatography has been used effectively in the purification of recombinant adeno-associated virus (Zolotukhin *et al.*, 1999). Iodixanol density gradient centrifugation has also been utilized in the purification

process of human respiratory syncytial virus to yield highly infectious virus particles (Gias *et al.*, 2008).

2 AIM OF THE STUDY

The aim of this study was to develop a purification protocol for CPV using chromatographic methods. Another objective was to label the purified capsids with fluorescent dyes in order to observe the infection process inside living cells using confocal microscope imaging. Additionally infection studies would be conducted to examine the infectivity of CPV particles after purification. Finally the purified capsids would be detected using atomic force microscopy (AFM) to elucidate the effectiveness of the purification protocol.

3 MATERIALS AND METHODS

3.1 Virus

3.1.1 Production of Concentrated CPV Medium

CPV type 2 (CPV-d) was grown in Nordon laboratory feline kidney (NLFK) cells for 7 days and then stored at -20ºC. The culture medium from infected cells was concentrated by ultrafiltration with a 500 kDa filter (Millipore). Concentrated virus medium was stored at -20ºC.

3.1.2 Empty CPV Capsids

CsCl gradient centrifugation was used to purify CPV and to create pure empty and full CPV capsids. Empty CPV capsids were used as a positive control in many experiments. The process took several hours to be completed. Final product was stored at +4ºC.

3.2 Anion Exchange Chromatography

DE-52 (diethylaminoethyl) was used as a matrix material. Size of the column was 7 cm (height) x 1.3 cm (width). The column was first washed with 30 ml 40 mM Tris pH 7. Then 4 ml concentrated CPV medium in 1:10 dilution in Dulbecco's modified Eagle's medium (DMEM) was added into the column followed by 30 ml 40mM Tris. The elution

was carried out by gradually increasing the NaCl-concentration of the buffer, from 0.05 M to 0.3 M NaCl in 40 mM Tris. The flow rate was 0.6 ml/min. Peristaltic pump P-1 (Pharmacia Biotech) was used to regulate the flow rate. Total of 20 or 25 fractions were taken, volume of 1.5 ml each. The fractions were then measured for their protein concentration at wavelength 280 nm using Nanodrop ND-1000 Spectrophotometer. Before the measurement the fractions were heated at +95 ºC for 6 minutes.

3.3 Concentration

Based on protein concentration measurement, certain fractions were combined and concentrated using Amicon Ultra 4 (Millipore) concentration tubes in Heraeus Megafuge 1.0R centrifuge with a 3360 rotor in 4000 g. After concentration, the combined fractions were washed with phosphate-buffered saline (PBS, 0.02 M sodium phosphate buffer with 0.15 M sodium chloride, pH 7.4) using the same tubes as in the concentration phase. All steps were performed at room temperature.

3.4 Size-exclusion Chromatography

Sepharose 4B (Pharmacia Biotech) was used as a matrix material. Size of the column was 23 cm (height) x 2 cm (width). The column was washed with 80-100 ml of PBS followed by the addition of the sample. The proteins were eluted with 50 ml of PBS at a flow rate of 1.5 ml/min. The flow rate was again controlled by peristaltic pump. Total of 25 fractions were taken, volume of 2 ml each. In some occasions, first and last fractions (1, 13-14) were taken as 10 ml fractions, so that total of 14 fractions was taken. The fractions were combined and concentrated, and their absorbance at 280 nm measured as previously.

3.5 Cation Exchange Chromatography

CM-Sepharose CL-6B was used as matrix material. Size of the column was 8.8 cm (height) x 1.3 cm (width). The column was first washed with 30 ml 0.02 M Na-phosphate buffer (pH 7). Next 4 ml concentrated CPV medium in 1:10 dilution in DMEM was added into the column and unbound proteins were washed with 25 ml 0.02 M Na-phosphate buffer. Proteins were eluted by gradually increasing the NaCl-concentration of the elution buffer, from 0.2 M to 0.8 M NaCl in 0.02 M Na-phosphate buffer. 12 fractions were taken, volume of 3 ml each. The flow rate was 0.6 ml/min and it was regulated by peristaltic pump. Fractions were measured for their absorbance as previously.

3.6 Dot Blot

Dot blot was used to specify the fractions that contained the virus. All steps were carried out at room temperature. Samples were pipetted on a nitrocellulose filter (Whatman) 1.5 µl at a time. Total volume per dot was 9 µl. Blocking solution of 5 % milk powder in Tris-buffered saline (TBS)-Tween (pH 7) was prepared and the blot was blocked for 1 hour. After blocking, the dot blot was kept in primary antibody solution for 45 minutes. Anti-capsid monoclonal antibody A3B10 (a gift from Colin Parrish) was used as a primary antibody in 1:400 dilution in 5 % milk powder-TBS-Tween. The blot was then washed for 5 minutes in TBS-Tween, total of 3 times followed by secondary antibody treatment for 30 minutes. Goat anti-mouse alkaline phosphatase conjugate (Bio-Rad) was used as a secondary antibody in 1:3000 dilution in 5 % milk powder-TBS-Tween. The blot was washed 3 times with TBS-Tween as previously. Detection was done with 50 µl NBT (nitroblue tetrazolium chloride) and 50 µl BCIP (5-bromo-4-chloro-3-indolylphosphate p-toluidine salt) in 5 ml APA buffer.

3.7 Sodium Dodecyl Sulfate Polyacrylamide Gel Electroforesis (SDS-PAGE)

SDS-PAGE was employed to determine the effectiveness of purification. The samples were prepared using 30-40 µl of virus fraction and 30-40 µl of loading buffer and the prepared samples were heated at 100ºC for 10 minutes. After denaturing the proteins, 40 µl of each sample were pipetted on the gel and the proteins were resolved in gel containing 15 % acrylamide. The gel was stained with Coomassie stain (0.04 % Serva Blue, 25 % isopropanol and 10 % CH_3COOH) for 10 minutes and washed with 10 % CH_3COOH until the protein bands were clearly visible.

3.8 Atomic Force Microscopy (AFM)

All AFM imaging was conducted under the guidance of my supervisor. Measurements were conducted with Dimension 3100 atomic force microscope and Nanoscope IV control unit. BS Multi 75 were used as tips. Specimens were prepared by pipetting 5 µl samples on the sample substrate and incubated for 5 minutes. Samples were then dried with nitrogen gas and washed with 20 µl PBS and dried as previously. Finally the samples were washed with nanopure water and dried again before imaging. Image sizes were 512 x 512 or 1024 x 1024 pixels. Scan rate was 0.5 – 1.5 Hz. Integral gain varied between 0.2 – 0.4 while proportional gain varied between 0.6 – 4.

3.9 Detection of Single CPV Particles

Coverslips were coated with 30 µl 0.01 % solution of poly-l-lysine (Sigma). After a couple of minutes, the coverslips were washed with PBS. After the coverslips were dried, 5 µl of (undiluted or in 1:5 or 1:10 dilution in PBS) purified CPV capsids (once with anion

exchange chromatography) were added and incubated for 20 minutes. Coverslips were then fixed and labeled as described in section 3.11 with A3B10 as a primary antibody (1:200 dilution in permeabilization buffer) and Alexa-555 as a secondary antibody (1:200 dilution in permeabilization buffer). For AFM, mica sheets were coated with poly-l-lysine using the same procedure as for coverslips. Then 5 µl of CPV fractions was added. The samples were dried and washed as described in section 3.8.

3.10 Fluorescent Labeling of CPV Particles

Chromatographically purified CPV capsids were labeled with Alexa-488-TFP-ester or Atto-488-NHS-ester. The concentration of the dye was 10 mg/ml in dimethylsulfoxide (DMSO). The dye was added in a 1:10 ratio to the capsid volume (7.5 µl of dye added to 75 µl of capsids). After the addition of the dye, the reaction was incubated for 1 h at room temperature. 10 µl of 1 M glycine was added for 10 minutes to stop the reaction. Unbound dye was separated from the conjugate by centrifugation in Nanosep 30 k Omega (Pall) tubes for several times with PBS using Heraeus Biofuge 13 centrifuge. NLFK cells were infected with labeled CPV and fixed at various time points post infection (p.i.).

3.11 Infection Studies

3.11.1 CPV Infection

NLFK cells were grown and maintained in Dulbecco's modified Eagle's medium (DMEM) supplemented with 10 % fetal bovine serum, 1 % antibiotics and 1 % non-essential amino acids.

After chromatographic purification, certain fractions had been combined and concentrated. These combined fractions were then diluted in DMEM. Next, 30 µl of virus dilution was added to each coverslip and incubated for 20 minutes at +37ºC. After the incubation, 2 ml of growth media was added and the cells were left at +37ºC. At different times post infection, the coverslips were rinsed with PBS and fixed with 4 % paraformaldehyde (PFA) in PBS for 20 minutes at room temperature. The coverslips were then washed with PBS and stored in PBS at +4ºC.

3.11.2 Immunolabeling

All steps were carried out at room temperature. The coverslips were first kept in permeabilization buffer (1 % BSA, 0.1 % Triton-X-100 and 0.01 % sodium azide in PBS) for 15 minutes followed by primary antibody (anti-NS1 monoclonal antibody) incubation (1:70 dilution in permeabilization buffer, 30 µl/coverslip) for 1 hour. The coverslips were then washed with permeabilization buffer, PBS and again with permeabilization buffer for 15 minutes each. The coverslips were then incubated with secondary antibody (goat anti-mouse immunoglobulin G-Alexa 555 or Alexa 488 conjugate, Molecular Probes) in 1:200 dilution in permeabilization buffer (30 µl/coverslip) for 30 minutes and kept in the dark. Finally the coverslips were rinsed with permeabilization buffer and PBS for 15 minutes each (in the dark) and embedded with Prolong Gold antifade reagent with DAPI (Molecular Probes) or Mowiol (Calbiochem) containing 30 mg/ml DABCO (Sigma).

3.12 Confocal Microscopy

All imaging was conducted with Olympus FluoView FV1000 confocal laser scanning microscope. Pixel time was 2 µs in all experiments.

Argon laser was used with excitation wavelength of 488 nm to view samples labeled with Alexa-488 or Atto-488. Emission was detected between 500-530 nm. In samples labeled with Alexa-555, HeNe laser was used with excitation wavelength of 543 nm. Emission wavelength ranged between 555-655 nm. Diode laser was used with excitation wavelength of 405 nm to view samples embedded with DAPI. Emission was detected between 425-475 nm.

Alexa-488 and Atto-488 conjugated CPV particles were visualized with 40x objective (UPLFLN 40x/1.30 oil). Sequential scanning was used. In Alexa-488 conjugated CPV imaging, used pixel size was 69 nm (zoom was 6). Image size was 512 x 512 pixels. Line averaging was 6 and pinhole size was 1 airy unit. When Atto-488 conjugated CPV particles were visualized, used pixel size was 620 nm and image size was 512 x 512 pixels. Line averaging was 6 and pinhole size was 1 airy unit.

Infectivity studies of purified CPV particles were conducted by taking 4-6 images of every sample and calculating the amount of infected cells in each image. Then, average value of infectivity was calculated for each fraction. Samples were visualized using 20x objective (UPLSAPO 20x/0.75). Pixel size was 1.2 µm and image size was 512 x 512 pixels. Line averaging was 4. Pinhole size was 2 airy units. The infectivity quantitation was performed with ImageJ software using “analyze particles” -function.

When visualizing single CPV particles, 60x objective (UPLSAPO 60x/1.35 oil). Pixel size was 69 nm (zoom 3) and image size was 1024 x 1024 pixels. Line averaging was 8 and pinhole size was 1 airy unit.

4 RESULTS

4.1 Purification

4.1.1 Double Anion Exchange Chromatography Followed by Size-exclusion Chromatography

Coarse separation of CPV capsids was carried out using anion exchange chromatography (**Fig. 3**). Starting material was 4 ml of concentrated virus medium. It was added to the DE-52 anion exchange column. Bound proteins were eluted by gradually increasing the NaCl concentration of the elution buffer. The flow rate was 0.6 ml/min. Most of the proteins were eluted in fractions 11, 12, 14 and 15, while the majority of CPV capsids were eluted in fractions 11-18 (**Fig. 3A** and **3B**). Fractions 13-18 have some impurities left according to SDS-PAGE (**Fig. 3A**).

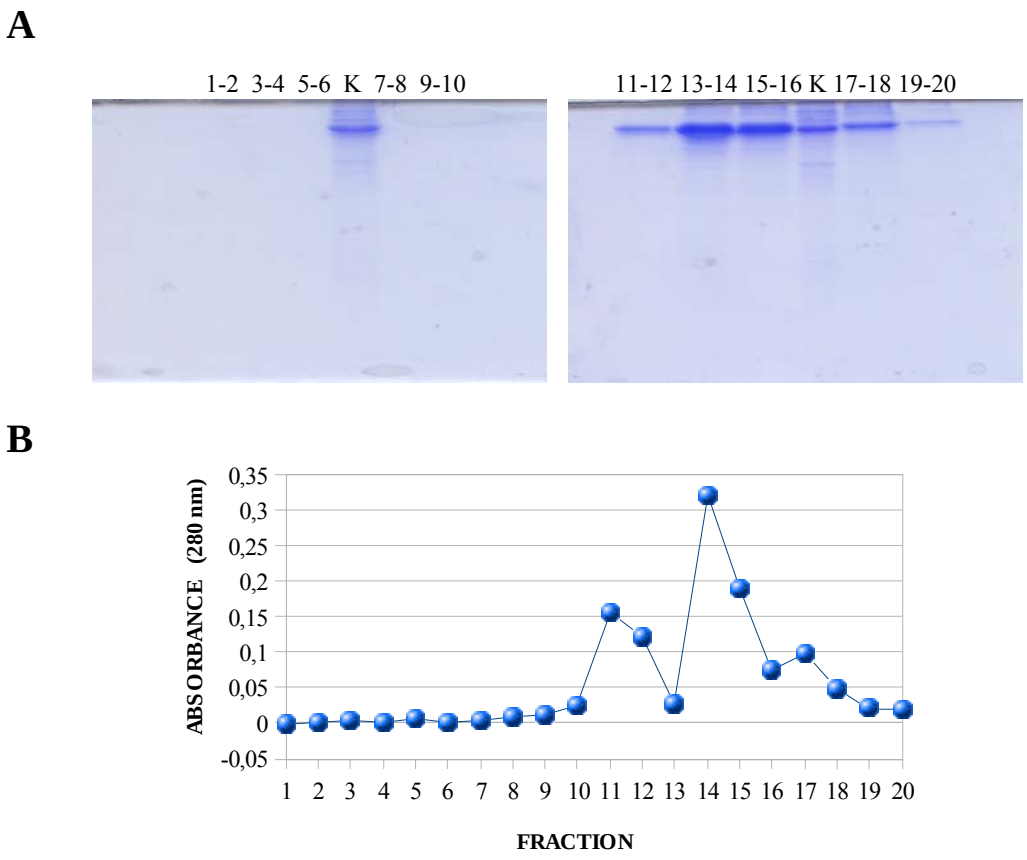

Fig. 3. First anion exchange chromatography. Numbers represent fractions. **(A)** 2 fractions were combined together as indicated by taking 30 µl from both fractions. Samples were not concentrated at this point. Samples (40 µl) and control (20 µl) were separated on a 15 % acrylamide gel. K = positive control (empty CPV capsids). **(B)** Elution profile of fractions 1-20. The graph represents absorbance at 280 nm.

To purify the capsids further, we used second round of anion exchange chromatography as a second step in purification (**Fig. 4**). Fractions 9-20 from the first anion exchange chromatography were combined and concentrated to a volume of about 1.20 ml and applied to the anion exchange column. As can be seen from the graph in **Fig. 4B**, most of the proteins were eluted in fractions 14, 15, 17 and 18 while the majority of CPV capsids were eluted in fractions 13-18 (**Fig. 4A**). Also, when looking at the SDS-PAGE, all fractions seem to be highly pure.

A

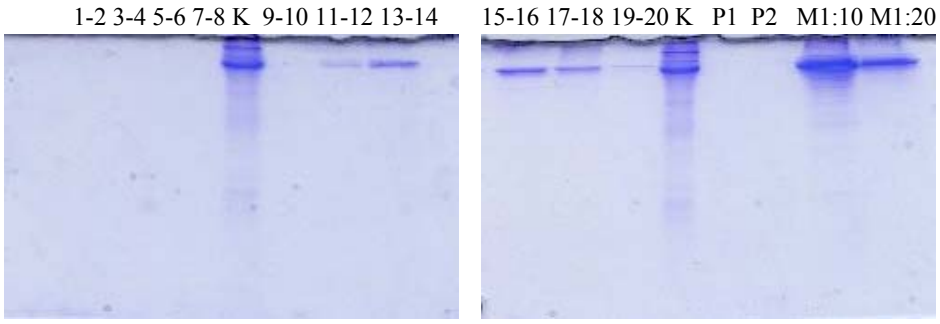

B

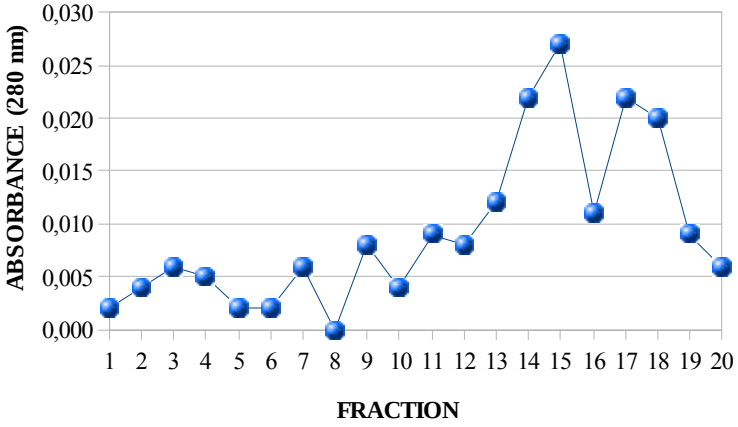

Fig. 4. Second anion exchange chromatography. Numbers represent fractions. **(A)** Fractions 9-20 from the first anion exchange chromatography were applied to the anion exchange column. Again, 2 fractions were combined but not concentrated by taking 30 µl of both fractions. Samples (40 µl) and control (20 µl) were separated on a 15 % acrylamide gel. K = positive control (empty CPV capsids). M1:10 = 1:10 dilution of the virus medium. M1:20 = 1:20 dilution of the virus medium. P1 was taken after the addition of the sample to the column and the following washing step with buffer. P2 was taken after the elution of the sample to see if any sample was left after collecting all of the fractions. **(B)** Absorbance of fractions 1-20 measured at 280 nm.

Fine purification of CPV capsids was performed using size-exclusion chromatography (**Fig. 5**). The optimal separation range for globular proteins using Sepharose 4B is 70 x 10^3 Da - 20 x 10^6 Da. Full CPV capsids have a molecular weight of 5.5 - 6.2 x 10^6 Da so it was expected that the capsids would be eluted rapidly, while the majority of cellular proteins would be hindered by the matrix and emerge much slower from the column.

Concentrated fractions 11-25 from the second anion exchange chromatography were applied to Sepharose 4B size-exclusion column. Fractions were eluted with PBS at a flow rate of 1.5 ml/min. As can be seen in **Fig. 5A**, the amount of the proteins has decreased so much that virtually no proteins can be seen in SDS-PAGE. The low concentration of proteins is also reflected on the absorbance values (**Fig. 5B**).

A

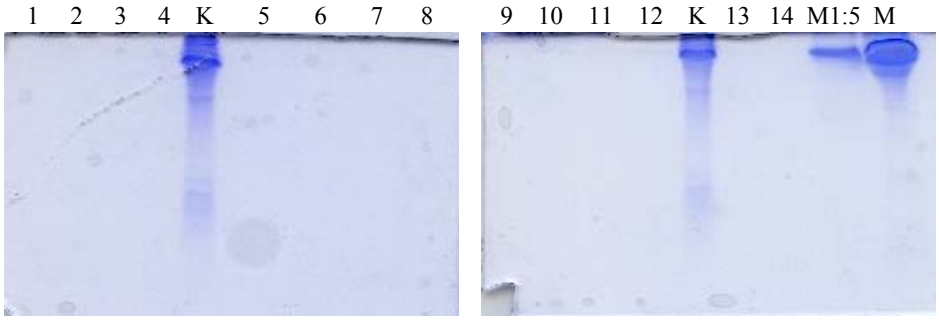

B

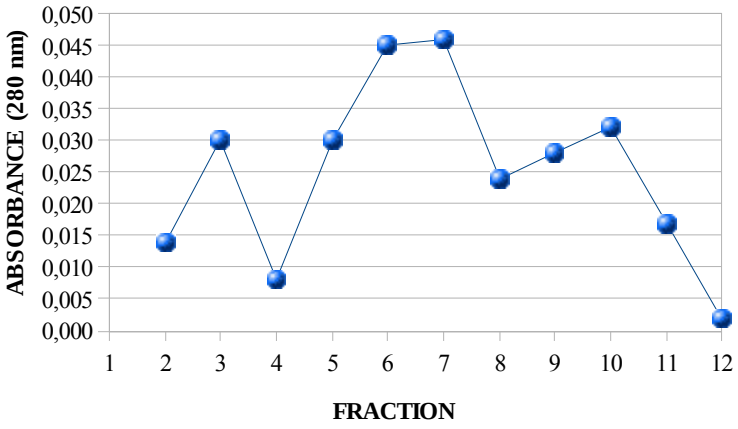

Fig. 5. Size-exclusion chromatography. Numbers represent fractions. **(A)** Fractions 11-25 from the second anion exchange chromatography were concentrated and added to the size-exclusion column. Fractions 1, 13 and 14 were taken as 10 ml fractions and have been concentrated to a volume of about 0.6 ml. Fractions 2-12 were unconcentrated. Samples (40 µl) and control (20 µl) were separated on a 15 % acrylamide gel. K = positive control (empty CPV capsids). M = virus medium that was applied to the first anion exchange column. M1:5 = 1:5 dilution of the virus medium. **(B)** Elution profile of eluted fractions 2-12. Absorbance was measured at 280 nm.

4.1.2 Anion Exchange Chromatography Followed by Size-exclusion Chromatography

Coarse separation of CPV capsids was again accomplished by anion exchange chromatography (**Fig. 6**). 4 ml of crudely purified and concentrated virus medium in 1:10 dilution was added to the anion exchange column and the fractions were eluted by increasing the NaCl concentration of the elution buffer. Fractions were collected and analyzed for the presence of CPV particles. Dot blot was used to specify the fractions that contained the virus, while SPS-PAGE was employed to determine the effectiveness of purification.

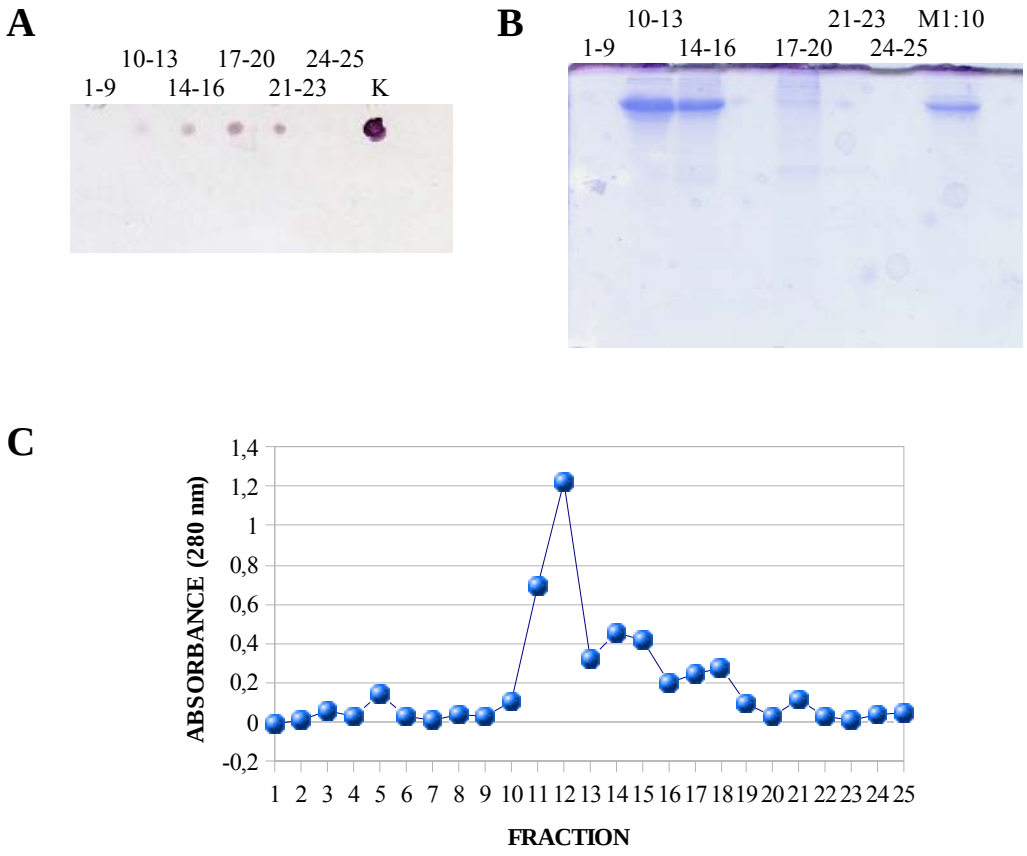

Fig. 6. Anion exchange chromatography. Numbers represent fractions. **(A)** Dot blot. Based on absorbance measurements, certain fractions have been combined and concentrated. Sample size was 9 µl/dot. K = positive control (empty CPV capsids). **(B)** SDS-PAGE of the combined and concentrated fractions. Samples (40 µl) and control (20 µl) were separated on a 15 % acrylamide gel. M1:10 = 1:10 dilution of the virus medium. **(C)** Elution profile of the fractions, absorbance measured at 280 nm.

Most of the proteins were eluted in fractions 11-13 (**Fig. 6C**), while the peak in CPV capsids appeared to be in fractions 14-23 (**Fig. 6A** and **6B**). According to the data in SDS-PAGE, there are still some unwanted proteins left in fractions 10-20 (**Fig. 6B**).

Fine purification of the capsids was carried out using size-exclusion chromatography (**Fig. 7**). Fractions 10-25 from the anion exchange chromatography were concentrated to a volume of about 1.75 ml and applied to the size-exclusion column. Most of the proteins were eluted in fractions 14-17 although the concentration of the proteins seems to be quite low (**Fig. 7C**). CPV capsids were mainly eluted in fractions 1-12 and trailed up to fractions 16-18 (**Fig. 7A**). SDS-PAGE shows considerably pure fractions, although no protein bands can be seen in fractions other than 13-18 (**Fig. 7B**).

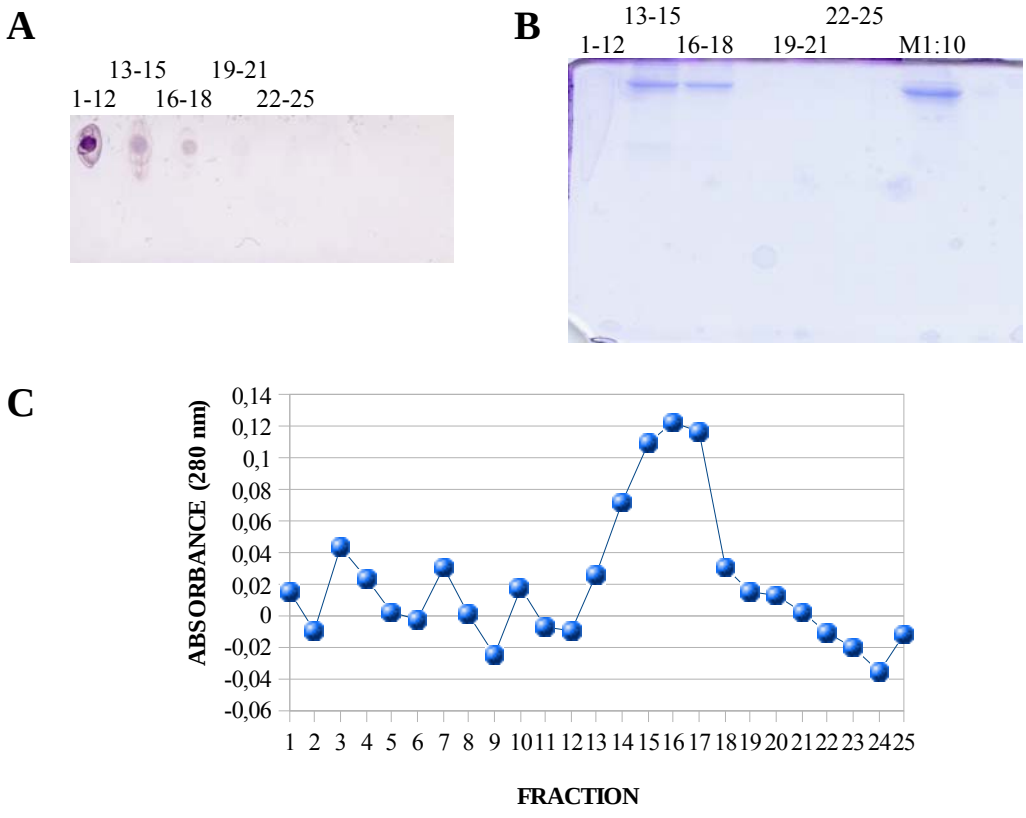

Fig. 7. Size-exclusion chromatography. Numbers represent fractions. **(A)** Dot blot. Certain fractions have been combined and concentrated based on absorbance measurement. Sample size was 9 µl/dot. **(B)** SDS-PAGE of the combined and concentrated fractions. Samples (40 µl) were separated on a 15 % acrylamide gel. M1:10 = 1:10 dilution of the virus medium. **(C)** Absorbance of the fractions measured at 280 nm.

4.1.3 Double Anion Exchange Chromatography

Anion exchange chromatography was employed to separate CPV capsids from other proteins in the virus medium (**Fig. 8**). Again, 4 ml of virus medium in 1:10 dilution was added to the column and eluted as previously. The peak in CPV elution seemed to be in fractions 11-13 trailing up to fractions 23-25 when looking at the dot blot data (**Fig. 8A**). According to the SDS-PAGE data, fractions 14-17 seemed to contain most of the CPV capsids (**Fig. 8B**). Fractions 17-20 seemed to be most impure.

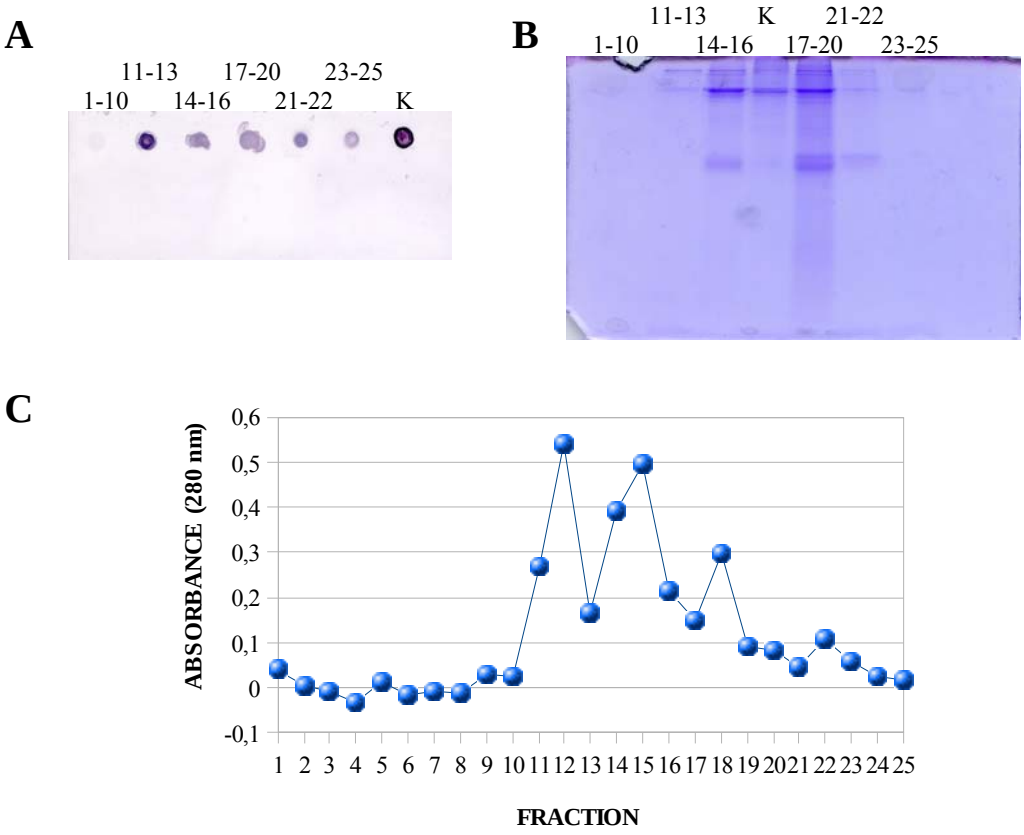

Fig. 8. First anion exchange chromatography. Numbers represent fractions. **(A)** Dot blot. Based on absorbance measurements, certain fractions have been combined and concentrated. Sample size was 9 µl/dot. K = positive control (empty CPV capsids). **(B)** SDS-PAGE of the combined and concentrated fractions. Samples (40 µl) and control (30 µl) were separated on a 15 % acrylamide gel. K = positive control (empty CPV capsids) **(C)** Elution profile of the fractions, absorbance measured at 280 nm.

To purify the capsids even further, second round of anion exchange chromatography was used (**Fig. 9**). Fractions 11-25 from the first anion exchange chromatography were combined and concentrated to a volume of about 1.1 ml and applied to the second anion exchange chromatography step. This time the peak in CPV elution seems to be in fractions 14-20 (**Fig. 9A**). Hardly any virus can be seen in fractions 21-23. There are still some impurities left, but as can be seen in SDS-PAGE, the concentration of proteins is very small (**Fig. 9B**). Also, the absorbance measured at 280 nm shows that the amount of the proteins is low.

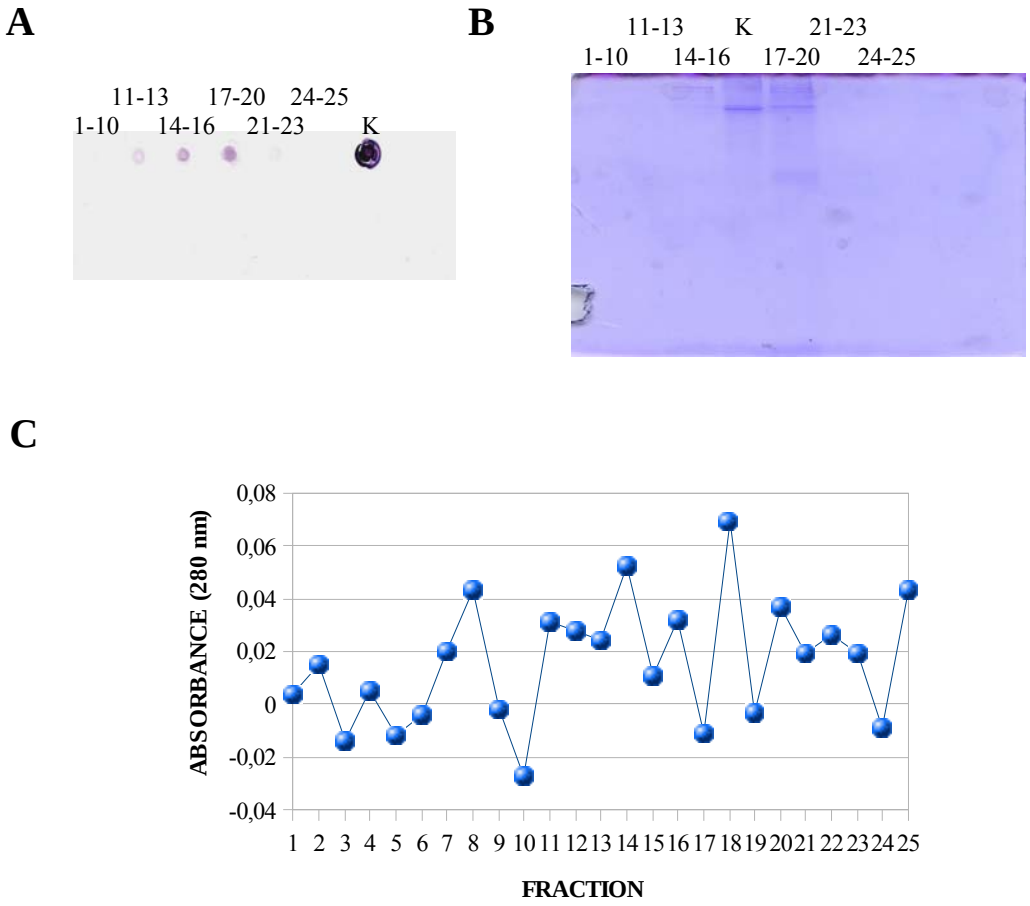

Fig. 9. Second anion exchange chromatography. **(A)** Dot blot. Based on absorbance measurements, certain fractions have been combined and concentrated. Sample size was 9 µl/dot. K = positive control (empty CPV capsids). **(B)** SDS-PAGE of the combined and concentrated fractions. Samples (40 µl) and control (30 µl) were separated on a 15 % acrylamide gel. K = positive control (empty CPV capsids) **(C)** Elution profile of the fractions, absorbance measured at 280 nm.

4.1.4 Anion Exchange Chromatography

Purification of CPV capsids was carried out using only anion exchange chromatography (**Fig. 10**). 2 ml of undiluted virus medium was added to the anion exchange column and the fractions were eluted by increasing the NaCl concentration of the elution buffer.

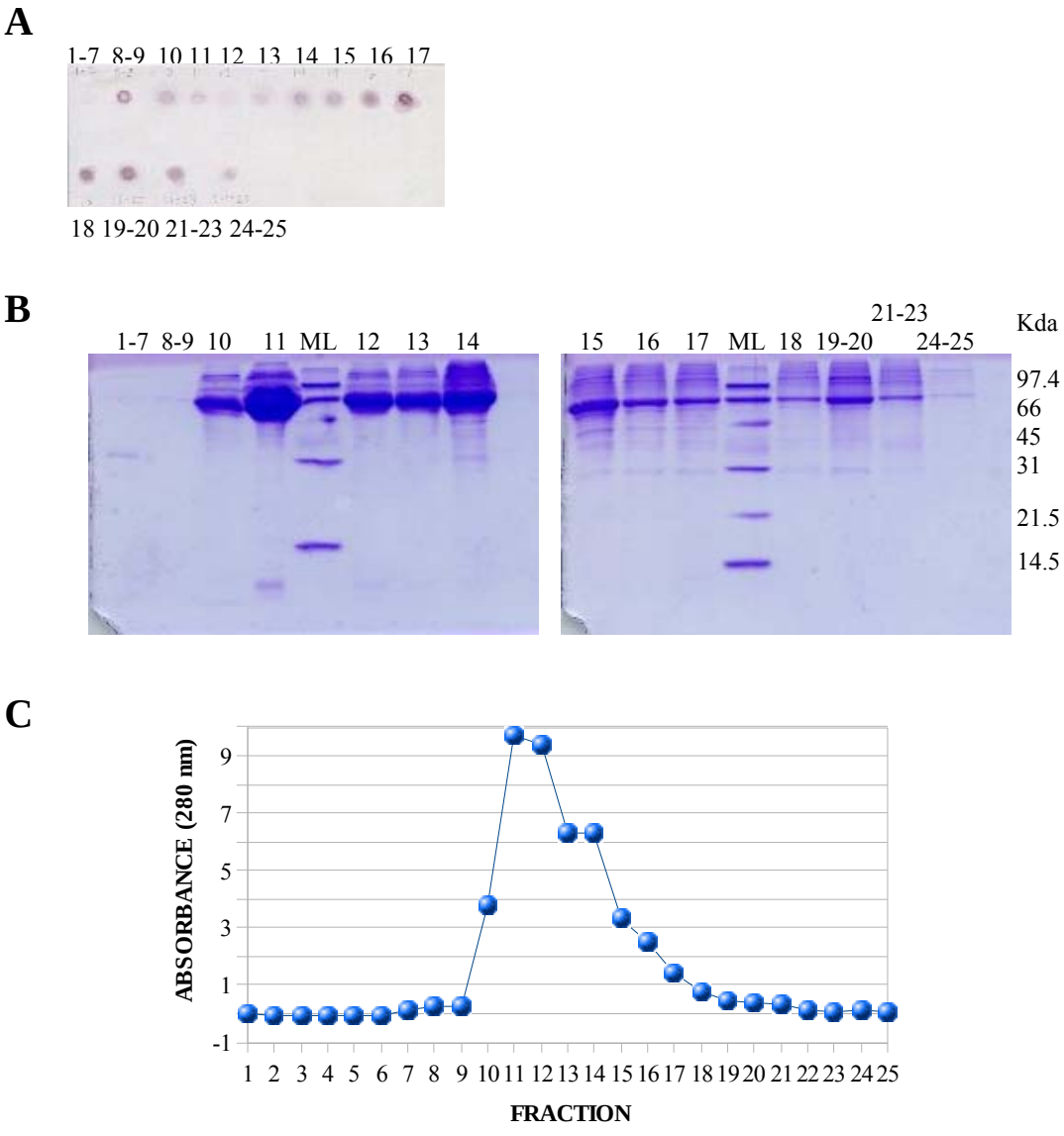

Fig. 10. Anion exchange chromatography. Numbers represent fractions. **(A)** Dot blot. Fractions were concentrated and pipetted on a nitrocellulose filter. Sample size was 9 µl/dot. **(B)** SDS-PAGE of the concentrated fractions. Samples (6 µl) and control (6 µl) were separated on a 15 % acrylamide gel. ML = Low molecular weight marker. Marker sizes are on the right of the figure. **(C)** Elution profile of the fractions, absorbance measured at 280 nm.

As can be seen in **Fig. 10A**, the virus was eluted in fractions 8-25, but fractions 11-13 and 24-25 seemed to contain only a minor portion of the virus. Most of the proteins were eluted in fractions 11-14 and these are also the fractions that contain most of the impurities (**Fig. 10B and 10C**).

4.1.5 Cation Exchange Chromatography

We wanted to investigate whether cation exchange chromatography could be used in the purification process of CPV (**Fig. 11**).

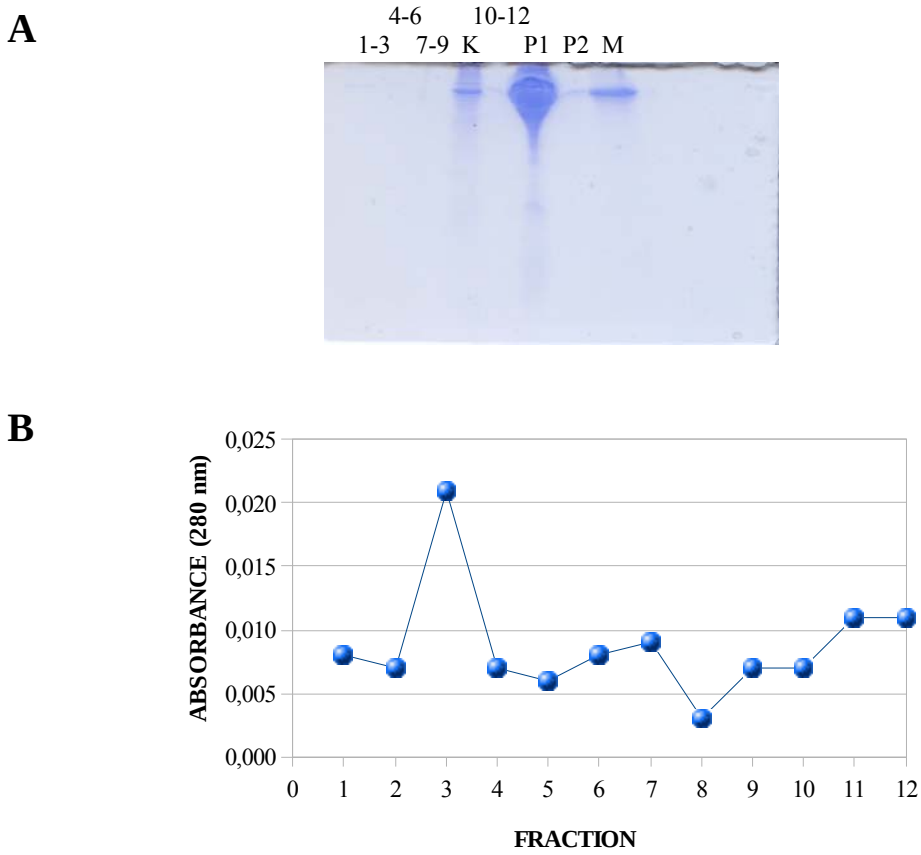

Fig. 11. Cation exchange chromatography. Numbers represent fractions. **(A)** SDS-PAGE was run from the fractions obtained from cation exchange chromatography. Based on absorbance measurement, certain fractions have been combined and concentrated. 20 µl samples and 15 µl control was applied to the gel. K = positive control (empty CPV capsids). P1 was taken after the addition of the sample to the column and the following washing step with buffer. P2 was taken after the elution of the sample to see if any sample was left after collecting all of the fractions. M=1:5 dilution of the medium. **(B)** Elution profile of the fractions, absorbance measured at 280 nm.

Unfortunately we found out that cation exchange chromatography was unsuccessful in the purification of CPV capsids, therefore it was not studied further. According to the data we obtained, most of the proteins were eluted in the first washing step before collecting the fractions (**Fig. 11A**). Also, as can be seen in **Fig. 11B**, the absorbance measured at 280 nm is very small.

4.2 Infectivity

NLFK cells were infected with chromatographically purified CPV particles and visualized using confocal microscopy to find out whether the purification protocol impairs the infectivity of the capsids. The fractions used in this experiment were purified once with anion exchange chromatography (**Fig. 10**). After anion exchange chromatography, certain fractions have been combined and concentrated. These combined fractions were then diluted and added on coverslips to infect NLFK cells. Infectivity studies of purified CPV particles were conducted by taking 4-6 images of every sample and calculating the amount of infected cells in each image. Then, average value of infectivity was calculated for each fraction. Fractions 10-13 were the most infective fraction: 23 % of the cells were infected while fractions 1-9 and 21-23 were the least infective (**Fig. 12**).

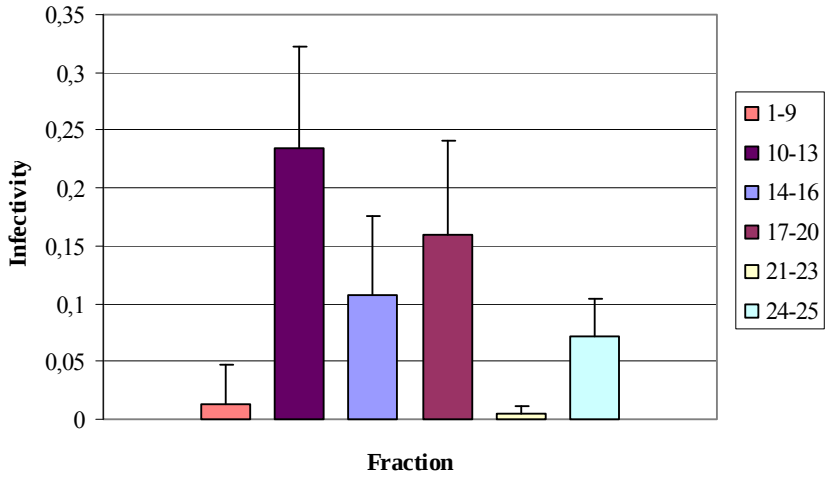

Fig. 12. Infectivity of fractions purified once with anion exchange chromatography. Thin lines represent standard deviation of each sample.

4.3 AFM and Confocal Microscopy Imaging of Chromatographically Purified CPV Particles

4.3.1 AFM Imaging of Purified CPV Capsids

AFM was used to determine the effectiveness of the purification protocols. AFM imaging showed dispersed, icosahedral particles with a diameter of approximately 50 nm. The difference between the starting material (virus medium) and the purified product (purified once with anion exchange chromatography) is obvious (**Fig. 13**). Purified virus particles can clearly be seen in both height and amplitude figures. When looking at the virus medium image, single virus particles are impossible to distinguish from other particles in the medium.

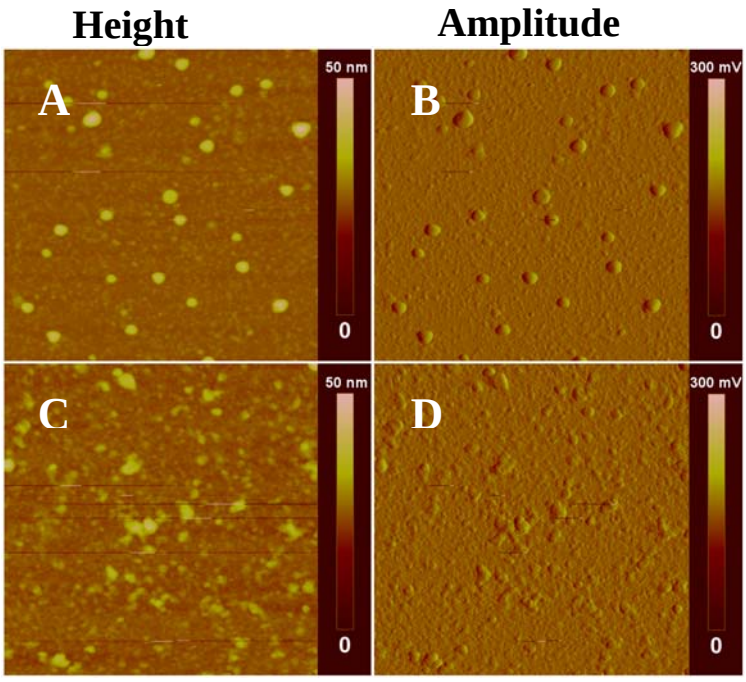

Fig. 13. AFM images of purified CPV capsids. **(A)** and **(B)** purified CPV particles. **(C)** and **(D)** virus medium (starting material for the purification). Scan area 1 x 1 µm.

CPV capsids purified with only anion exchange chromatography appeared as highly pure, single particles when examined with AFM. On the other hand, when the virus capsids were observed after size-exclusion chromatography, large pieces of unknown material can be seen in addition to the virus particles in both height and amplitude images (**Fig. 14**).

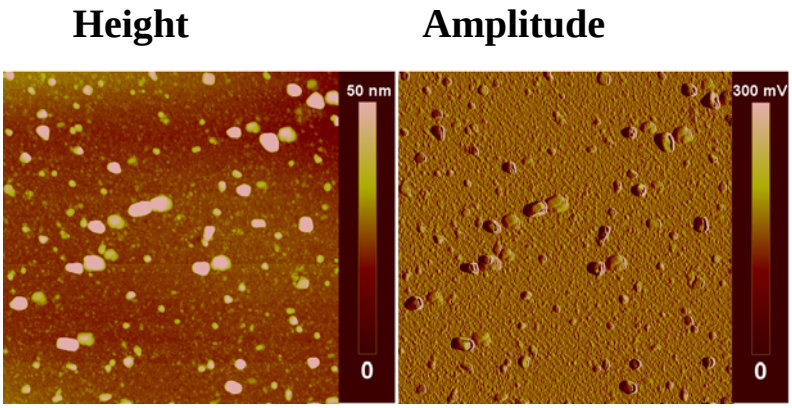

Fig. 14. AFM imaging of CPV particles after anion exchange chromatography and size-exclusion chromatography. Scan area 1 x 1 µm.

4.3.2 Detection of Single CPV Particles

CPV capsids purified with anion exchange chromatography were attached to coverslips coated with poly-l-lysine in an attempt to visualize single CPV particles using confocal microscopy. Confocal microscopy images showed small, round particles with a fluorescent label (**Fig. 15**). Intensity of the fluorescence varied between the particles. AFM imaging confirmed that CPV particles actually are dispersed as single virus particles (**Fig. 16**).

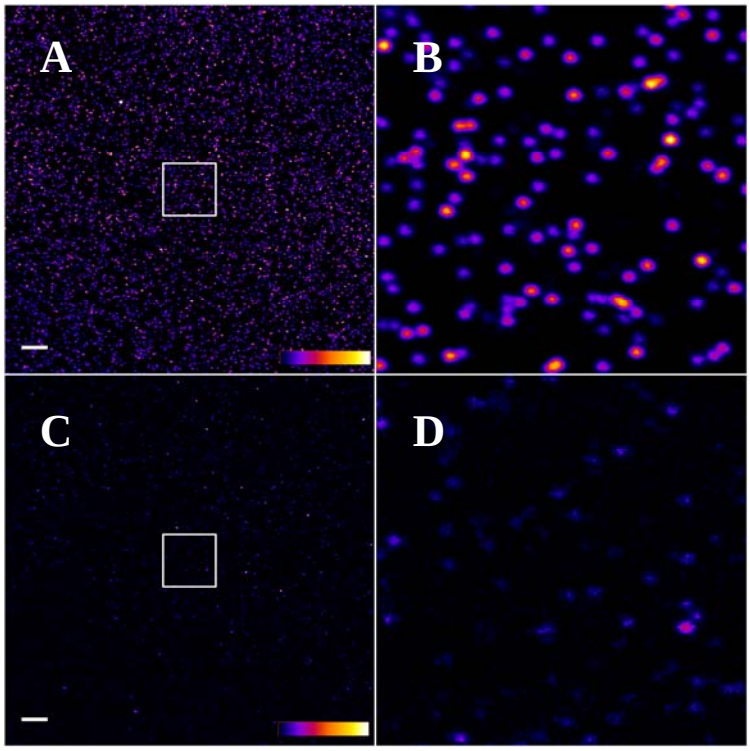

Fig. 15. Confocal microscopy imaging of single CPV particles. Coverslips were coated with poly-l-lysine, and chromatographically purified CPV was added. CPV particles were fixed in 4 % PFA and immunolabeled with A3B10. Finally, CPV particles were imaged by Olympus FluoView FV1000. **(A)** CPV capsids after single anion exchange chromatography. **(B)** Magnification of the boxed area in fig. A. **(C)** Image was taken outside the area where the capsids were pipetted. (**D)** Magnification of the boxed area in fig. C. Scale bars 5 µm. White boxes 10 µm x 10 µm. The colored bars represent intensity of fluorescence between values 0 – 255.

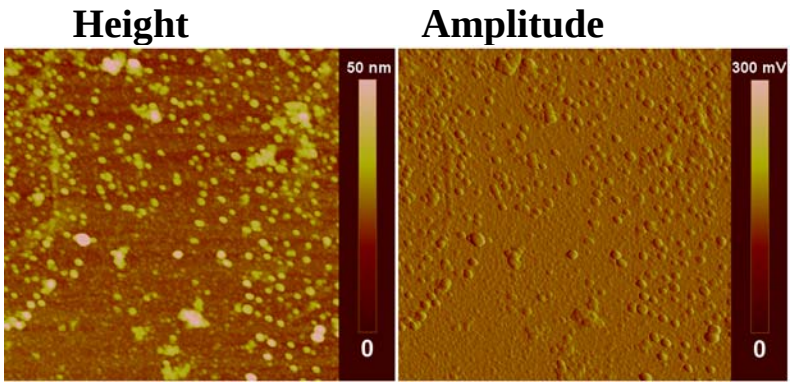

Fig. 16. AFM imaging of CPV particles purified with anion exchange chromatography. Sample substrate was coated with poly-l-lysine and dried before 5 µl of purified CPV capsids were added. Scan area 1 x 1 µm.

4.4 Fluorescent Labeling of CPV Capsids

The attempt to conjugate Atto-488-NHS-ester or Alexa-488-TFP-ester to chromatographically purified CPV capsids failed. Although the labeling failed, CPV particles remain infective as can be seen in **Fig**. **17** and **18**.

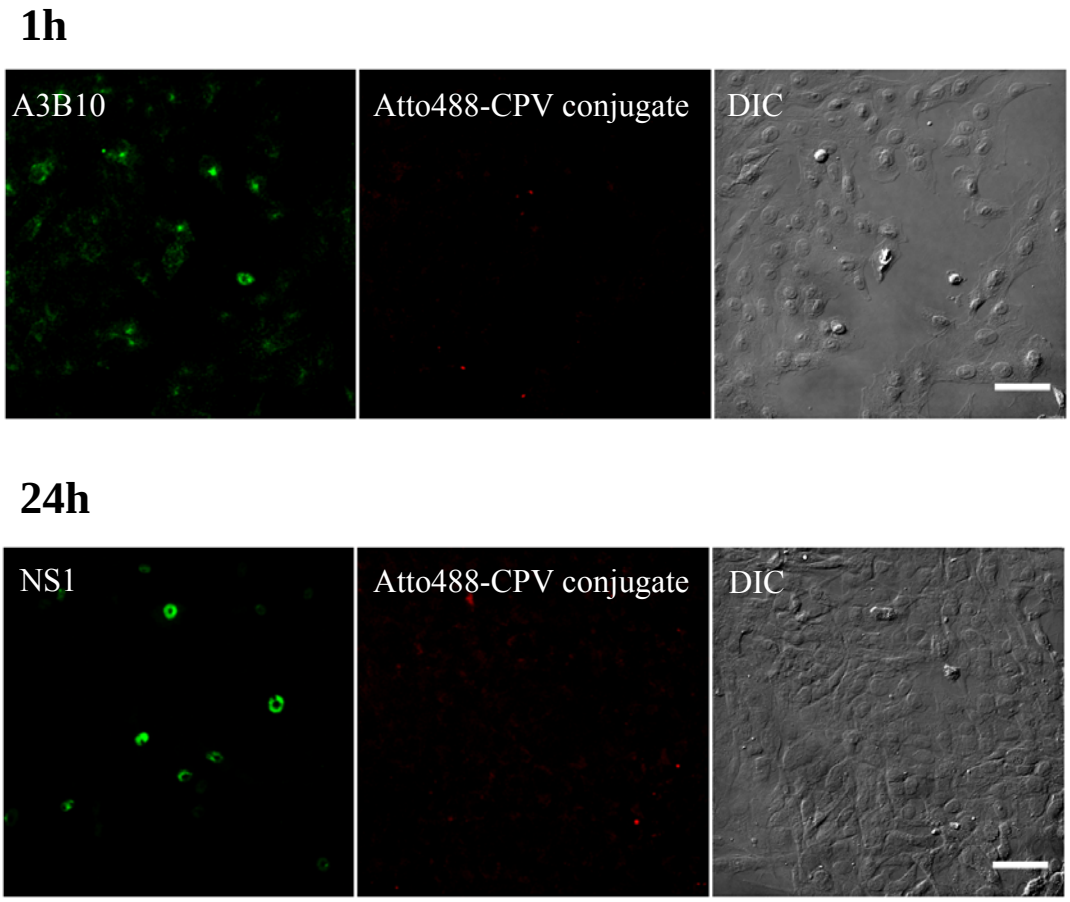

Fig. 17. Atto-488 conjugated CPV. Chromatographically purified CPV capsids were conjugated with Atto-488-NHS-ester. NLFK cells were infected with these labeled capsids (1:7.5 dilution) and immunolabeled with A3B10 (1h p.i.) or anti-NS1 monoclonal antibody (24 h p.i.). Scale bars 50 µm.

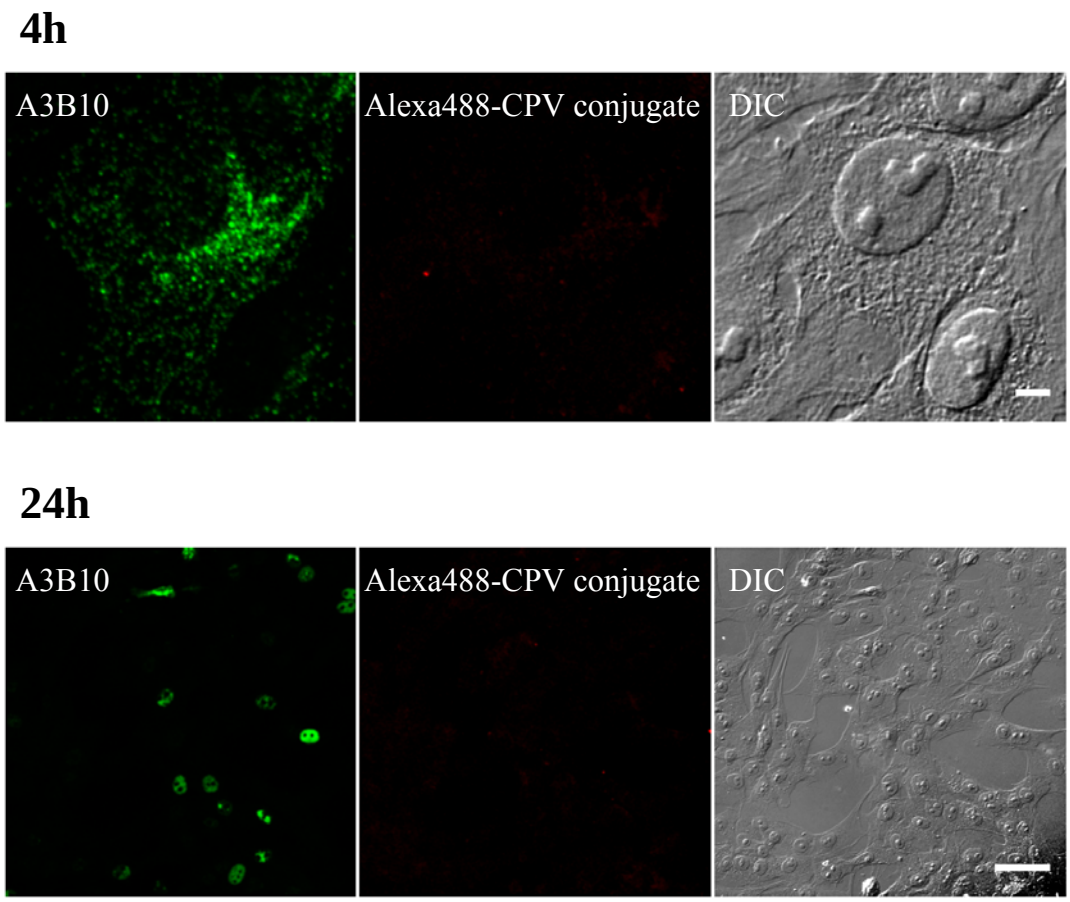

Fig. 18. Alexa-488 conjugated CPV. Chromatographically purified CPV capsids were conjugated with Alexa-488-TFP-ester. NLFK cells were infected with these labeled capsids (1:7.5 dilution) and immunolabeled with A3B10 (4h p.i.) or anti-NS1 monoclonal antibody (24 h p.i.) Scale bar in 4h image 5 µm. Scale bar in 24 h image 50 µm.

5 DISCUSSION

5.1 The Examination of the Purification Techniques and Characterization of the Purified CPV Particles

Many research groups have recently been developing new methods for virus purification that would allow them to acquire pure viral particles with higher yield than when the traditional CsCl gradients are being used (Zolotukhin *et al.*, 1999; O'Riordan *et al.*, 2000; Smith *et al.*, 2003; Davidoff *et al.*, 2004; Kamen and Henry, 2004; Duffy *et al.*, 2005; Segura *et al.*, 2005; Kalbfuss *et al.*, 2007; Koerber *et al.*, 2007; Rodrigues *et al.*, 2007). CsCl-based techniques are known to be detrimental to the infectivity of the virus, thus new methods were needed to ensure that the virus remains infective after the purification process. Additionally, chromatographic purification is much faster than CsCl gradient centrifugation.

We investigated five possible chromatographic methods for purification of CPV particles (**Fig. 19**). After trying out different combinations of size-exclusion and anion exchange chromatography, we concluded that the best results were obtained when only one round of anion exchange chromatography was used. Our first plan had three chromatography phases (**Fig. 3-5**). We used two rounds of anion exchange chromatography to eliminate most of the unwanted proteins, and the final purification step was conducted by size-exclusion chromatography. It can be seen from the SDS-PAGE that these techniques produce highly purified virus, but the amount of the virus decreases with each purification step. To increase the yield of the purified virus, we decided to exclude the second anion exchange chromatography phase (**Fig. 6-7**). Again, highly purified virus was produced according to SDS-PAGE, but when the fractions were examined with AFM large amounts of impurities were detected in fractions after size-exclusion chromatography. We believe that these

impurities are pieces of the matrix material of the size-exclusion chromatography column. This could be explained by the age of the column; it is possible that the matrix is getting to the end of its life and it would be best to replace it with a fresh one. However, this is something we have to consider in future experiments.

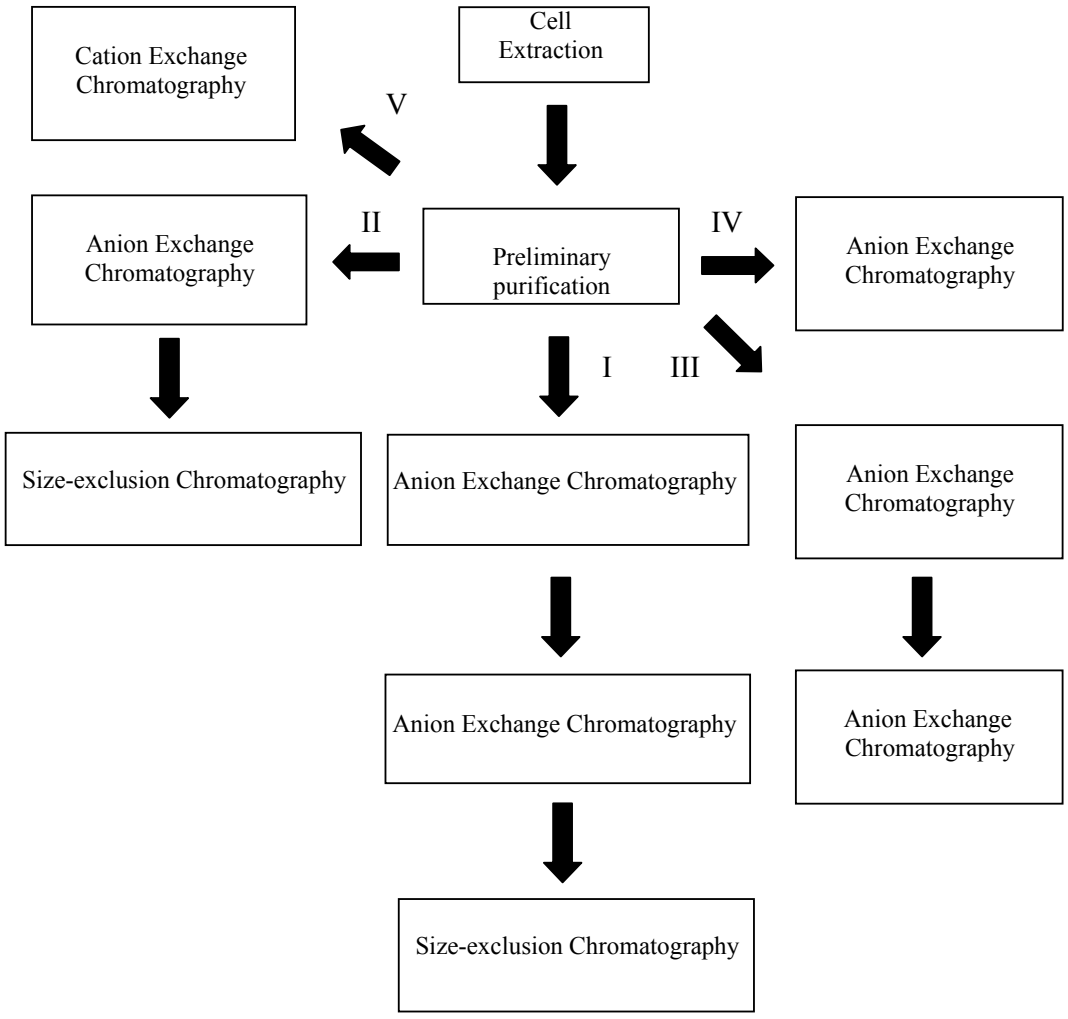

Fig. 19. The flow chart illustrates the chromatographic steps in CPV purification that were investigated in this study.

Because of the problems with the size-exclusion chromatography matrix, we decided to use only anion exchange chromatography. At first our plan was to use double anion exchange chromatography (**Fig. 8-9**), but as the concentration of proteins decreased

considerably, we decided to skip the second anion exchange chromatography step (**Fig. 10**). It can be seen from the SDS-PAGE and AFM (**Fig. 13A-B**) that only one anion exchange chromatography is enough to produce pure CPV capsids. We also tried cation exchange chromatography in order to separate CPV particles from the rest of the proteins, but as can be seen in **Fig. 11**, this technique failed. The reason for the failure can be explained by looking at the isoelectric point of CPV capsids: the isoelectric point of CPV particles is 5.3 pH which makes the capsids negatively charged at neutral pH (Weichert *et al.*, 1998), thus the capsids tend to elute rather quickly with the rest of the proteins.

When looking at the figures from first anion exchange chromatography (**Fig. 4, 6, 8** and **10**), one can come to a conclusion that CPV capsids are eluted after the majority of the proteins have been eluted from the column (after the absorbance peak that can be seen in the absorbance graph in **Fig. 3B, 6C, 8C** and **10C**). Although some CPV capsids are eluted in fractions that contain most of the proteins, majority of CPV capsids tend to elute in fairly pure fractions. By adjusting the elution step, we would be able to elute the capsids in a more compact volume, and to exclude even more of the unwanted proteins from the CPV fractions.

We also discovered that for some reason, some absorbance measurements gave negative values, which was unexpected (**Fig. 3B, 6C, 7C, 8C, 9C** and **10C**). This could result from using 40 mM Tris without NaCl as a blank when measuring the absorbance of fractions obtained from anion exchange chromatography. However, this does not explain why we acquired negative values from some of the fractions from size-exclusion chromatography (**Fig. 7C**). Most probably this is a technical issue caused by the spectrophotometer.

5.2 Infectivity

Our infectivity studies showed that CPV capsids remain infective after chromatographic purification. The reason for the difference in the infectivity values between the different

fractions can be explained by variable concentration of CPV particles in each fraction. The most infective fractions were 17-20 in relation to the absorbance value (**Fig. 10** and **12**). Although fractions 10-13 had the greatest absolute infectivity, they contained most of the impurities as well.

5.3 Fluorescent Labeling of CPV Capsids

The procedure for conjugating Alexa or Atto dyes to CPV capsids failed (**Fig. 17-18**) most likely due to low concentration of the virus in the reaction. It is recommended that the protein concentration in the reaction should be more than 2 mg/ml, otherwise the efficiency of the reaction will greatly decrease. We suspect that the protein concentration in our experiment was less than 2 mg/ml, which explains the failure. If this method would have been successful, it would have allowed us to investigate the infection process in more detail by observing the intracellular route and dynamics of CPV in living cells. It would have also been possible to study co-localization between CPV and different organelles and molecules in real time in cells.

5.4 Conclusions

Chromatographic purification of CPV is indeed an excellent way of obtaining pure and infective CPV particles. The procedure is fast and simple, and it can easily be scaled up to produce more purified virus. Optimization is still needed in order to allow the capsids to be eluted in a more compact volume from the anion exchange column. Also, the next step is automatization of the whole purification procedure, consequently making the purification process more convenient.

REFERENCES

Agbandje, M., C.R. Parrish, and M.G. Rossmann. 1995. The structure of parvoviruses. *Semin Virol.* 6:299-309.

Agbandje-McKenna, M., A.L. Llamas-Saiz, F. Wang, P. Tattersall, and M.G. Rossmann. 1998. Functional implications of the structure of the murine parvovirus, minute virus of mice. *Structure.* 6:1369-1381.

Buonavoglia, C., V. Martella, A. Pratelli, M. Tempesta, A. Cavalli, D. Buonavoglia, G. Bozzo, G. Elia, N. Decaro, and L. Carmichael. 2001. Evidence of canine parvovirus type 2 in Italy. *J Gen Virol.* 82:3021-3025.

Burova, E., and E. Ioffe. 2005. Chromatographic purification of recombinant adenoviral and adeno-associated viral vectors: methods and implications. *Gene Ther.* 12:S5-S17.

Chang, S.-F., J.-Y. Sgro, and C.R. Parrish. 1992. Multiple amino acids in the capsid structure of canine parvovirus coordinately determine the canine host range and specific antigenic and hemagglutination properties. *J Virol.* 66:6858-6867.

Chapman, M.S., and M.G. Rossmann. 1995. Single-stranded DNA-protein interactions in canine parvovirus. *Structure.* 3:151-162.

Cortes, E., C. San Martin, J. Langeveld, R. Meloen, K. Dalsgaard, C. Vela, and I. Casal. 1993. Topographical analysis of canine parvovirus virions and recombinant VP2 capsids. *J Gen Virol.* 74:2005-2010.

Cotmore, S.F., and P. Tattersall. 2007. Parvoviral host range and cell entry mechanisms. *Adv Virus Res.* 70:184-232.

Davidoff, A.M., C.Y.C. Ng, S. Sleep, J. Gray, S. Azam, Y. Zhao, J.H. McIntosh, M. Karimipoor, and A.C Nathwani. 2004. Purification of recombinant adeno-associated virus type 8 vectors by ion exchange chromatography generates clinical grade vector stock. *J Virol Methods.* 121:209-215.

Decaro, N., C. Desario, M. Campolo, G. Elia, V. Martella, D. Ricci, E. Lorusso, and C. Buonavoglia. 2005. Clinical and virological findings in pups naturally infected by canine parvovirus type 2 glu-426 mutant. *J Vet Diagn Invest.* 17:133-138.

Duffy, A.M., A.M. O'Doherty, T. O'Brien, and P.M. Strappe. 2005. Purification of adenovirus and adeno-associated virus: comparison of novel membrane-based technology to conventional techniques. *Gene Ther.* 12:S62-S72.

Gias, E., S.U. Nielsen, L.A.F. Morgan, and T.L. Toms. 2008. Purification of human respiratory syncytial virus by ultracentrifugation in iodixanol density gradient. *J Virol Methods.* 147:328-332.

Govindasamy, L., K. Hueffer, C.R. Parrish, and M. Agbandje-McKenna. 2003. Structures of host range-controlling regions of the capsids of canine and feline parvoviruses and mutants. *J Virol.* 77:12211-12221.

Horiuchi, M., Y. Yamaguchi, T. Gojobori, M. Mochizuki, H. Nagasawa, Y. Toyoda, N. Ishiguro, and M. Shinagawa. 1998. Differences in the evolutionary pattern of feline panleukopenia virus and canine parvovirus. *Virology.* 249:440-452.

Hueffer, K., J.S.L. Parker, W.S. Weichert, R.E. Geisel, J.-Y. Sgro, and C.R. Parrish. 2003a. The natural host range shift and subsequent evolution of canine parvovirus resulted from virus-specific binding to the canine transferrin receptor. *J Virol.* 77:1718-1726.

Hueffer, K., L. Govindasamy, M. Agbandje-McKenna, and C.R. Parrish. 2003b. Combinations of two capsid regions controlling canine host range determine transferrin receptor binding by canine and feline parvoviruses. *J Virol.* 77:10099-10105.

Hueffer, K., L.M. Palermo, and C.R. Parrish. 2004. Parvovirus infection of cells by using variants of the feline transferrin receptor altering clathrin-mediated endocytosis, membrane domain-localization, and capsid-binding domains. *J Virol.* 78:5601-5611.

Hurtado, A., P. Rueda, J. Nowicky, J. Sarraseca, and J.I. Casal. 1996. Identification of domains in canine parvovirus VP2 essential for the assembly of virus-like particles. *J Virol.* 70:5422-5429.

Kalbfuss, B., M.Wolff, R. Morenweiser, and U. Reichl. 2007. Purification of cell culture-derived human influenza A virus by size-exclusion and anion-exchange chromatography. *Biotechnol Bioeng.* 96:932-944.

Kamen, A., and O. Henry. 2004. Development and optimization of an adenovirus production process. *J Gene Med.* 6:S184-S192.

Koerber, J.T., J.-H. Jang, J.H. Yu, R.S Kane, and D.V. Schaffer. 2007. Engineering adeno-associated virus for one-step purification via immobilized metal affinity chromatography. *Hum Gene Ther.* 18:367-378.

Langeveld, J.P.M., J.I. Casal, C. Vela, K. Dalsgaard, S.H. Smale, W.C. Puijk, and R.H. Meloen. 1993. B-cell epitopes of canine pavovirus: distribution on the primary structure and exposure on the viral surface. *J Virol.* 67:765-772.

Llamas-Saiz, A.L., M. Agbandje-McKenna, J.S.L. Parker, A.T.M. Wahid, C.R. Parrish and M.G. Rossmann. 1996. Structural analysis of a mutation in canine parvovirus which controls antigenicity and host range. *Virology.* 225:65-71.

Martyn, J.C., B.E. Davidson, and M.J. Studdert. 1990. Nucleotide sequence of feline panleukopenia virus: comparison with canine parvovirus identifies host-specific differences. *J Gen Virol.* 71:2747-2753.

López de Turiso, J.A., E. Cortés, A. Ranz, J. García, A. Sanz, C. Vela, and J.I. Casal. 1991. Fine mapping of canine parvovirus B cell epitopes. *J Gen Virol.* 72:2445-2456.

López de Turiso, J.A., E. Cortés, C. Martínez, R. Ruiz de Ybáñez, I. Simarro, C. Vela, and I. Casal. 1992. Recombinant vaccine for canine parvovirus in dogs. *J Virol.* 66:2748-2753.

O'Riordan, C.R., A.L. Chapelle, K.A. Vincent, and S.C. Wadsworth. 2000. Scaleable chromatographic purification process for recombinant adeno-associated virus (rAAV). *J Gene Med.* 2:444-454.

Palermo, L.M., K. Hueffer, and C.R. Parrish. 2003. Residues in the apical domain of the feline and canine transferrin receptors control host-specific binding and cell infection of canine and feline parvoviruses. *J Virol.* 77:8915-8923.

Palermo, L.M., S.L. Hafenstein, and C.R. Parrish. 2006. Purified feline and canine transferrin receptors reveal complex interactions with the capsids of canine and feline parvoviruses that correspond to their host ranges. *J Virol.* 80:8482-8492.

Paradiso, P.R., S.L. Rhode III, and I.I. Singer. 1982. Canine parvovirus: a biochemical and ultrastructural characterization. *J Gen Virol.* 62:113-125.

Parker, J.S.L., and C.R. Parrish. 1997. Canine parvovirus host range in determined by the specific conformation of an additional region of the capsid. *J Virol.* 71:9214-9222.

Parker, J.S.L., and C.R. Parrish. 2000. Cellular uptake and infection by canine parvovirus involves rapid dynamin-regulated clathrin-mediated endocytosis, followed by slower intracellular trafficking. *J Virol.* 74:1919-1930.

Parker, J.S.L., W.J. Murphy, D. Wang, S.J. O'Brien, and C.R. Parrish. 2001. Canine and feline parvoviruses can use human or feline transferrin receptors to bind, enter, and infect cells. *J Virol.* 75:3896-3902.

Parrish, C.R., P. Have, W.J. Foreyt, J.F. Evermann, M. Senda, and L.E. Carmichael. 1988. The global spread and replacement of canine parvovirus strains. *J Gen Virol.* 69:1111-1116.

Parrish, C.R. 1990. Emergence, natural history, and variation of canine, mink, and feline parvoviruses. *Adv Virus Res.* 38:403-450.

Parrish, C.R., C.F. Aquadro, M.L. Strassheim, J.F. Evermann, J.-Y. Sgro, and H.O. Mohammed. 1991. Rapid antigenic-type replacement and DNA sequence evolution of canine parvovirus. *J Virol.* 65:6544-6552.

Pérez, R., L. Francia, V. Romero, L. Maya, I. López, and M. Hernández. 2007. First detection of canine parvovirus type 2c in South America. *Vet Microbiol.* 124:147-152.

Reed, A.P., E.V. Jones, and T.J. Miller. 1988. Nucleotide sequence and genome organization of canine parvovirus. *J Virol.* 62:266-276.

Rhode III, S.L. 1985. Nucleotide sequence of the coat protein gene of canine parvovirus. *J Virol.* 54:630-633.

Riolobos, L., J. Reguera, M.G. Mateu, and J.M. Almendral. 2006. Nuclear transport of trimeric assembly intermediates exerts a morphogenetic control on the icosahedral parvovirus capsid. *J Mol Biol.* 357:1026-1038.

Rodrigues, T., A. Carvalho, M. Carmo, M.J.T. Carrondo, P.M. Alves, and P.E. Cruz. 2007. Scaleable purification process for gene therapy retroviral vectors. *J Gene Med.* 9:233-243.

Saliki, J.T., B. Mizak, H.P. Flore, R.R. Gettig, J.P. Burand, L.E. Carmichael, H.A. Wood, and C.R. Parrish. 1992. Canine parvovirus empty capsids produced by expression in a baculovirus vector: use in analysis of viral properties and immunization of dogs. *J Gen Virol.* 73:369-374.

Segura, M.M., A. Kamen, P. Trudel, and A. Garnier. 2005. A novel purification strategy for retrovirus gene therapy vectors using heparin affinity chromatography. *Biotechnol Bioeng.* 90:391-404.

Smith, R.H., C. Ding, and R.M. Kotin. 2003. Serum-free production and column purification of adeno-associated virus type 5. *J Virol Methods.* 114:115-124.

Steinel, A., C.R. Parrish, M.E. Bloom, and U. Truyen. 2001. Parvovirus infections in wild carnivores. *J Wildl Dis.* 37:594-607.

Suikkanen, S., K. Sääjärvi, J. Hirsimäki, O. Välilehto, H. Reunanen, M. Vihinen-Ranta, and M. Vuento. 2002. Role of recycling endosomes and lysosomes in dynein-dependent entry of canine parvovirus. *J Virol.* 76:4401-4411.

Suikkanen, S., T. Aaltonen, M. Nevalainen, O. Välilehto, L. Lindholm, M. Vuento, and M. Vihinen-Ranta. 2003a. Exploitation of microtubule cytoskeleton and dynein during parvoviral traffic toward the nucleus. *J Virol.* 77:10270-10279.

Suikkanen, S., M. Antila, A. Jaatinen, M. Vihinen-Ranta, and M. Vuento. 2003b. Release of canine parvovirus from endocytic vesicles. *Virology.* 316:267-280.

Tratschin, J.-D., G.K. McMaster, G. Kronauer, and G. Siegl. 1982. Canine parvovirus: relationship to wild-type and vaccine strains of feline panleukopenia virus and mink enteritis virus. *J Gen Virol.* 61:33-41.

Tresnan, D.B., L. Southard, W. Weichert, J.-Y. Sgro, and C.R. Parrish. 1995. Analysis of the cell and erythrocyte binding activities of the canine parvovirus capsid. *Virology.* 211:123-132.

Truyen, U., and C.R. Parrish. 1992. Canine and feline host ranges of canine parvovirus and feline panleukopenia virus: distinct host cell tropisms of each virus in vitro and in vivo. *J Virol.* 66:5399-5408.

Truyen, U., A. Gruenberg, S.-F. Chang, B. Obermaier, P. Veijalainen, and C.R. Parrish. 1995. Evolution of the feline-subgroup parvoviruses and the control of canine host range in vivo. *J Virol.* 69:4702-4710.

Tsao, J.T., M.S. Chapman, M. Agbandje, W. Keller, K. Smith, H. Wu, M. Luo, T.J. Smith, M.G. Rossmann, R.W. Compans, and C.R. Parrish. 1991. The three-dimensional structure of canine parvovirus and its functional implications. *Science.* 251:1456-1464.

Vihinen-Ranta, M., L. Kakkola, A. Kalela, P. Vilja, and M. Vuento. 1997. Characterization of a nuclear localization signal of canine parvovirus capsid proteins. *Eur J Biochem.* 250:389-394.

Vihinen-Ranta, M., A. Kalela, P. Mäkinen, L. Kakkola, V. Marjomäki, and M. Vuento. 1998. Intracellular route of canine parvovirus entry. *J Virol.* 72:802-806.

Vihinen-Ranta, M., W. Yuan, and C.R. Parrish. 2000. Cytoplasmic trafficking of the canine parvovirus capsid and its role in infection and nuclear transport. *J Virol.* 74:4853-4859.

Vihinen-Ranta, M., D. Wang, W.S. Weichert, and C.R. Parrish. 2002. The VP1 N-terminal sequence of canine parvovirus affects nuclear transport of capsids and efficient cell infection. *J Virol.* 76:1884-1891.

Vihinen-Ranta, M., S. Suikkanen, and C.R. Parrish. 2004. Pathways of cell infection by parvoviruses and adeno-associated viruses. *J Virol.* 78:6709-6714.

Wang, D., W. Yuan, I. Davis, and C.R. Parrish. 1998. Nonstructural protein-2 and the replication of canine parvovirus. *Virology.* 240:273-281.

Weichert, W.S., J.S.L. Parker, A.T.M. Wahid, S.-F. Chang, E. Meier, and C.R. Parrish. Assaying for structural variation in the parvovirus capsid and its role in infection. *Virology.* 250:106-117.

Xie, Q., and M.S. Chapman. 1996. Canine parvovirus capsid structure, analyzed at 2.9 Å resolution. *J Mol Biol.* 264:497-520.

Yuan, W., and C.R. Parrish. 2001. Canine parvovirus capsid assembly and differences in mammalian and insect cells. *Virology.* 279:546-557.

Zolotukhin, S., B.J. Byrne, E. Mason, I. Zolotukhin, M. Potter, K. Chesnut, C. Summerford, R.J. Samulski, and N. Muzyczka. 1999. Recombinant adeno-associated virus purification using novel methods improves infectious titer and yield. *Gene Ther.* 6:973-985.